

# Meta Curvature-Aware Minimization for Domain Generalization

Ziyang Chen<sup>1</sup> Yiwen Ye<sup>1</sup> Feilong Tang<sup>2</sup> Yongsheng Pan<sup>1†</sup> Yong Xia<sup>1,3,4†</sup>

<sup>1</sup> School of Computer Science and Engineering, Northwestern Polytechnical University, China

<sup>2</sup> Faculty of Engineering, Monash University, Australia

<sup>3</sup> Research & Development Institute of Northwestern Polytechnical University in Shenzhen, China

<sup>4</sup> Ningbo Institute of Northwestern Polytechnical University, China

{zychen, ywye}@mail.nwpu.edu.cn, feilong.tang@monash.edu, {yspan, yxia}@nwpu.edu.cn

## Abstract

Domain generalization (DG) aims to enhance the ability of models trained on source domains to generalize effectively to unseen domains. Recently, Sharpness-Aware Minimization (SAM) has shown promise in this area by reducing the sharpness of the loss landscape to obtain more generalized models. However, SAM and its variants sometimes fail to guide the model toward a flat minimum, and their training processes exhibit limitations, hindering further improvements in model generalization. In this paper, we first propose an improved model training process aimed at encouraging the model to converge to a flat minima. To achieve this, we design a curvature metric that has a minimal effect when the model is far from convergence but becomes increasingly influential in indicating the curvature of the minima as the model approaches a local minimum. Then we derive a novel algorithm from this metric, called **Meta Curvature-Aware Minimization (MeCAM)**, to minimize the curvature around the local minima. Specifically, the optimization objective of MeCAM simultaneously minimizes the regular training loss, the surrogate gap of SAM, and the surrogate gap of meta-learning. We provide theoretical analysis on MeCAM’s generalization error and convergence rate, and demonstrate its superiority over existing DG methods through extensive experiments on five benchmark DG datasets, including PACS, VLCS, OfficeHome, TerraIncognita, and DomainNet. Code will be available on [GitHub](#).

## 1. Introduction

In recent years, deep neural networks (DNNs) have demonstrated significant success across various computer vision tasks [1, 2, 49]. However, models trained on source data

<sup>†</sup>Corresponding author.

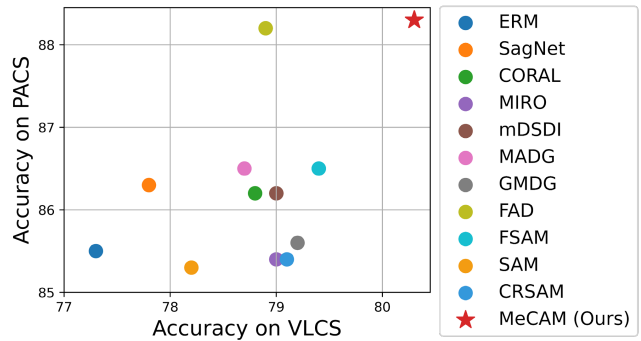


Figure 1. Accuracy of our MeCAM and existing DG methods on the PACS and VLCS datasets. MeCAM achieves superior generalization performance on both datasets.

often experience performance degradation when applied to unseen target domains due to distribution shifts [63]. This limitation hinders the practical deployment of these models in real-world scenarios.

Domain generalization (DG) has emerged as a promising approach to address this challenge by leveraging source data to train models that generalize well to new, unseen domains. Several DG techniques have been developed to improve model generalization, including domain alignment [37, 50], data augmentation [74, 84], ensemble learning [45, 54], and disentangled representation learning [58, 72], and so on.

Despite these advancements, simply minimizing standard loss functions, such as cross-entropy loss, often fails to achieve satisfactory generalization [20], as it may result in a sharp loss landscape. Recent research [22, 25, 29] has explored the relationship between the geometry of the loss landscape and model generalization. Sharpness-aware minimization (SAM) and its variants [20, 42, 75, 76, 89] have shown that reducing the sharpness of the loss landscape leads to improved generalization. These sharpness-based methods generally optimize the model by perturbing its parameters within a small radius, aiming to find flatter regions

in the loss landscape.

While SAM has been successful in achieving flatter loss landscapes, it exhibits limitations in representing sharpness. Specifically, SAM measures sharpness based on the loss value, whereas sharpness itself is independent of the loss value. Moreover, SAM aims to reduce sharpness consistently, even when the model is not yet close to a local minimum. We argue that the model training process should follow two key principles: (1) focus on minimizing the loss when the model is far from convergence, and (2) shift the focus to reducing sharpness as the model approaches a local minimum. This approach is more reasonable, as unconverged models do not require sharpness consideration, and sharpness should not be dependent on the loss value.

To address these issues, we first introduce a curvature metric that adheres to these principles. This metric is independent of the loss value and effectively measures the curvature around local minima. As the model converges, the metric increases, reflecting the curvature of the loss landscape. Our goal is to minimize both this curvature metric and the vanilla training loss to train a model with better generalization ability. Building on this, we propose a novel sharpness-based algorithm, Meta Curvature-Aware Minimization (MeCAM), which jointly minimizes the surrogate gap of SAM and meta-learning to find a flatter minima for better generalization. The optimization objective of MeCAM incorporates the vanilla training loss, the surrogate gap of SAM, and the surrogate gap of meta-learning. Minimizing the training loss leads the model toward a local minimum, while minimizing the other two terms reduces the curvature, thereby improving generalization. MeCAM encourages the model to converge to a flatter region, enhancing its generalization ability (see Figure 1).

The contributions of this work are three-fold. (1) We analyze the limitations of SAM and introduce principles for a more effective training process. We propose a curvature metric that better represents sharpness than SAM. (2) We introduce the MeCAM algorithm, which jointly minimizes the surrogate gap of SAM and meta-learning to find a flatter minima. (3) Extensive experiment results on five DG datasets demonstrate that MeCAM outperforms existing DG methods, achieving superior generalization performance.

## 2. Related Work

### 2.1. DG Methods

DG methods [73, 87] aim to train models on source data in a way that enables them to generalize well to other out-of-distribution data. Existing DG approaches can be broadly categorized into four groups based on their methodology and motivation: (1) domain alignment [37, 44, 50, 65, 68], which measures the distance between distinct distributions

and learns domain-invariant representations to enhance the robustness of the model; (2) data augmentation [12, 74, 84, 85], which strongly enhances the diversity of training data to prevent the model from over-fitting to the training data; (3) ensemble learning [45, 51, 54, 86], which trains multiple models and uses their ensemble to improve predictions and reduce bias; and (4) disentangled representation learning [58, 59, 72], which separates features into domain-variant and domain-invariant components, using the domain-invariant features for more robust predictions. Although these DG methods have achieved significant success in improving model generalization, they may still underperform on out-of-distribution data due to a lack of constraints on the sharpness of the loss landscape. In this paper, we introduce a novel sharpness-based approach to guide the model toward a flatter minima, further enhancing generalization.

### 2.2. SAM in DG

The connection between the sharpness of the loss landscape and generalization ability has been explored in earlier studies [15, 22, 25, 29]. For instance, Dinh *et al.* [15] suggested that the sharpness of a local minima is related to the Hessian spectrum, with the eigenvalues of the Hessian matrix reflecting the curvature of the loss landscape. Recent advancements in SAM and its variants [16, 20, 35, 46, 75, 76, 83, 89] have shown that flatter minima are associated with better generalization. SAM [3, 20] uses worst-case perturbations of model weights to force the model to converge to a flatter minima, thereby improving generalization. Zhuang *et al.* [89] and Wang *et al.* [75] focus on optimizing the gap between the perturbation loss in SAM and the vanilla training loss. Wu *et al.* [76] present the normalized Hessian trace as a regularizer for SAM to counter excessive non-linearity of loss landscape and compute the trace via finite differences. In contrast, our approach derives a new optimization objective from a curvature metric, which offers a more precise measure of the sharpness around the local minima. We then derive the optimization objective of jointly minimizing the surrogate gap of SAM and meta-learning from minimizing this metric, facilitating the search for a flatter minima with better generalization performance.

### 2.3. Meta-learning in DG

Meta-learning [27, 30], also known as learning-to-learn, focuses on leveraging knowledge from related tasks to improve learning on new tasks. Recent studies have introduced meta-learning techniques into the domain generalization setting, enabling models to generalize across diverse domains by identifying patterns that are transferable to unseen domains. Finn *et al.* [19] proposed a meta-learning approach that divides the training data into meta-train and meta-test sets, training the model to boost its performance

on the meta-test set. Li *et al.* [39] introduced a model-agnostic training procedure that simulates distribution shifts by synthesizing virtual test domains. Balaji *et al.* [5] applied meta-learning by encoding domain generalization as a regularization function, learning a generalized regularizer to guide the training process. In this paper, we propose MeCAM, which enhances the conventional meta-learning with SAM to guide the model toward a flatter minima, thereby further improving its generalization performance.

### 3. Methodology

#### 3.1. Preliminaries

##### 3.1.1 Problem Definition

Let  $\theta \in \mathbb{R}^k$  represent the model parameters, where  $k$  is the parameter dimension. We denote the training datasets as  $\mathcal{D} = \{\mathcal{D}_i\}_i^S$ , consisting of  $S$  datasets, each containing  $n_i$  training samples, denoted by  $\{(x_i^j, y_i^j)\}_{j=1}^{n_i} \sim \mathcal{D}_i$ , where  $x_i^j$  and  $y_i^j$  are the input data and corresponding target labels, respectively. The training loss function over the dataset  $\mathcal{D}$  is defined as  $f(\theta; \mathcal{D})$ , based on cross-entropy loss. For simplicity, we denote  $f(\theta; \mathcal{D})$  as  $f(\theta)$  unless otherwise specified. The first derivative and the Hessian matrix of  $f(\theta)$  at point  $\theta$  are denoted by  $\nabla f(\theta)$  and  $H(\theta)$ , respectively. We use  $\|\cdot\|$  to represent the L2 norm throughout the paper.

##### 3.1.2 Objective of SAM

Conventional optimization of DNNs typically minimizes the training loss  $f(\theta)$  using gradient descent, but this often leads to sharp local minima, which can hinder generalization performance [89]. To address this issue, SAM [20] aims to find a flatter region in the loss landscape where the model parameters are robust to small perturbations. The objective of SAM can be formulated as:

$$\min_{\theta} f(\theta + \delta), \quad \delta = \rho \frac{\nabla f(\theta)}{\|\nabla f(\theta)\| + \epsilon} \quad (1)$$

where  $\delta$  denotes the perturbation,  $\rho$  controls the perturbation radius, determining the amplitude of the perturbation, and  $\epsilon$  is a small constant to avoid division by zero.

#### 3.2. Curvature Metric

Since SAM measures sharpness based solely on the loss value, it may fail to accurately capture the true sharpness in some situations [75, 83, 89]. As shown in Figure 2 (a), a smaller  $f(\theta^{sam})$  does not always guarantee a flatter minima. Additionally, SAM consistently minimizes sharpness during training, without considering that the model should focus on minimizing the loss during early stages of training and only reduce sharpness near local minima. We propose a more rational training process that follows two principles:

(1) minimize the loss when the model is far from convergence; and (2) reduce the sharpness when the model approaches a local minimum. Inspired by [18], we define a curvature metric that is independent of the loss value and adheres to these principles, providing a more accurate measure of sharpness and improving the model’s training process, as shown in Figure 2 (b). The curvature metric is formulated as:

$$\mathcal{C}(f(\theta)) = \frac{H(\theta)}{\|\nabla f(\theta)\|^2 + 1}. \quad (2)$$

This metric plays a minor role when the model is far from convergence but becomes more significant as the model approaches a local minimum. We also explore the relationship between the curvature metric and the maximal eigenvalue of the Hessian,  $\lambda_{max}(H(\theta))$ , which is a proper measure of the sharpness of the local minima [28, 29] and is related to the generalization ability of the model [11]. Although  $\lambda_{max}(H(\theta))$  is challenging to approximate and optimize directly [78, 83], we derive the following lemma showing that our curvature metric serves as a suitable surrogate for  $\lambda_{max}(H(\theta))$ .

**Lemma 3.1.** *Suppose that  $\|\mathcal{C}(f(\theta))\|$  is sub-multiplicative. Then, we have*

$$\lambda_{max}(H(\theta)) = \|\mathcal{C}(f(\theta))\| \cdot \|\|\nabla f(\theta)\|^2 + 1\|. \quad (3)$$

The proof can be found in Supplementary Material A.

#### 3.3. Meta Curvature-Aware Minimization

As  $\theta$  approaches a local minimum, the gradient  $\nabla f(\theta)$  in Eq. (2) inevitably decreases. Consequently, we minimize the Hessian to reduce  $\mathcal{C}$ . Based on this analysis, we propose the MeCAM framework, which optimizes the following overall objective:

$$\min_{\theta} f(\theta) + H(\theta), \quad (4)$$

where minimizing  $f(\theta)$  helps  $\theta$  approach the local minima, and minimizing  $H(\theta)$  focuses on reducing the curvature around the local minima.

Calculating  $H(\theta)$  for a large matrix, such as a DNN with millions of parameters, is computationally expensive. To reduce complexity, we approximate  $H(\theta)$  using the central difference method:

**Theorem 3.2.** *Suppose  $f(\theta)$  is twice-differentiable at  $\theta$ . Using the central difference method, we have*

$$H(\theta) = \frac{f(\theta + h) + f(\theta - h) - 2f(\theta)}{h^2} + O, \quad (5)$$

where  $h$  is a small step-size, and  $O$  denotes the remainder term. We estimate  $H(\theta)$  by calculating finite differences at symmetric neighboring points around the point of interest.

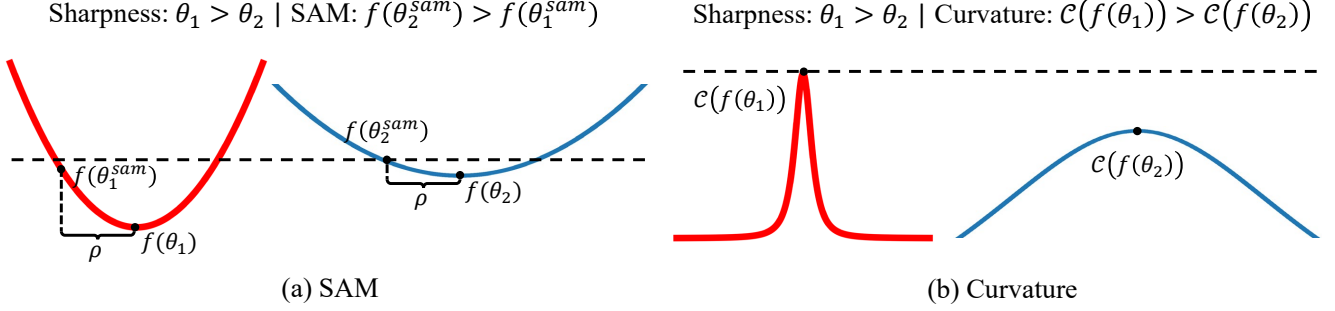


Figure 2. Comparison between SAM and the proposed curvature metric. (a) Illustration of a sharp local minimum at  $\theta_1$  (red) and a flat local minimum at  $\theta_2$  (blue). While SAM prefers to optimize around  $\theta_2^{sam}$ ,  $\theta_2$  is inherently flatter than  $\theta_1$ . This highlights SAM’s limitation in accurately characterizing sharpness, as it is influenced by the loss value. (b) Illustration of the proposed curvature metric  $\mathcal{C}$ . Unlike SAM,  $\mathcal{C}$  more effectively quantifies the deviation from a flat surface, providing a better measure of sharpness in the loss landscape. A smaller value of  $\mathcal{C}$  indicates a flatter minimum. Best viewed in color.

By incorporating information from both sides, this approach can provide an accurate approximation of  $H(\theta)$ . A key consideration in Eq. (5) is the choice of  $h$ . Common strategies for choosing an appropriate value of  $h$  include balancing round-off errors, adjusting based on the scale of the problem, using typical small constants, and so on [14, 55]. To avoid additional computation, in this study, we empirically set

$$h = \delta = \rho \frac{\nabla f(\theta)}{\|\nabla f(\theta)\| + \epsilon}, \quad (6)$$

$$\frac{1}{h^2} = \alpha,$$

where  $\alpha$  is a hyperparameter. The objective in Eq. (4) can then be rewritten as:

$$\min_{\theta} f(\theta) + \alpha(f(\theta + \delta) - f(\theta)) + \alpha(f(\theta - \delta) - f(\theta)). \quad (7)$$

**Generalization analysis.** Here we derive a generalization bound based on PAC-Bayesian theorem [48] for our MeCAM in Proposition 3.3.

**Proposition 3.3.** *Suppose the loss function  $f$  is differentiable and bounded by  $M$ , and the training set consists of  $n$  i.i.d. samples drawn from the true distribution. Let  $\hat{f}(\theta)$  represent the loss on the training set. Let  $\theta \in \mathbb{R}^k$  be learned from the training set with a number of  $k$ . Then, with probability at least  $1 - \zeta$ , we have*

$$\mathbb{E}_{\delta_i \sim \mathcal{N}(0, \sigma^2)} [f(\theta + \delta)] \leq \hat{f}(\theta) + \alpha(\hat{f}(\theta + \delta) + \hat{f}(\theta - \delta) - 2\hat{f}(\theta)) + \frac{M}{\sqrt{n}} + \sqrt{\frac{\frac{1}{4}k \log(1 + \frac{\|\theta\|^2(1 + \sqrt{\frac{\ln n}{k}})^2)}{\rho^2}) + \frac{1}{4} + \log \frac{n}{\zeta} + 2 \log(6n + 3k)}{n - 1}}. \quad (8)$$

It implies that  $f(\theta)$  is bounded by  $\hat{f}(\theta) + \alpha(\hat{f}(\theta + \delta) + \hat{f}(\theta - \delta) - 2\hat{f}(\theta))$  when ignoring high-order terms, and

minimizing the second term in the right side of Eq. (8) is expected to tighten the upper bound, rendering  $\alpha(\hat{f}(\theta + \delta) + \hat{f}(\theta - \delta) - 2\hat{f}(\theta))$  a regularization term controlled by the hyperparameter  $\alpha$ .

**Convergence analysis.** We analyze the convergence rate of MeCAM under the assumption that  $f$  is  $L$ -Lipschitz smooth.

**Theorem 3.4.** *Suppose  $f(\theta)$  is  $L$ -Lipschitz smooth. For any time-step  $t$  and  $\theta \in \Theta$ , suppose we can observe  $g_t$ ,  $g_t^{sam}$ , and  $g_t^{meta}$  as the gradients of  $\nabla f(\theta_t)$ ,  $\nabla f(\theta_t + \delta)$ , and  $\nabla f(\theta_t - \delta)$ , with  $\|g_t\|, \|g_t^{sam}\|, \|g_t^{meta}\| \leq G$ . Then, with learning rate  $\eta_t = \frac{\eta_0}{\sqrt{t}}$  and perturbation radius  $\rho_t = \frac{\rho_0}{\sqrt{t}}$ , we have*

$$\frac{1}{T} \sum_{t=1}^T \|\nabla f(\theta_t)\|^2 \leq \frac{C_1 + C_2 \log T}{\sqrt{T}},$$

$$\frac{1}{T} \sum_{t=1}^T \|\nabla f(\theta_t + \delta_t)\|^2 \leq \frac{C_3 + C_4 \log T}{\sqrt{T}}, \quad (9)$$

$$\frac{1}{T} \sum_{t=1}^T \|\nabla f(\theta_t - \delta_t)\|^2 \leq \frac{C_5 + C_6 \log T}{\sqrt{T}},$$

where  $C_1, C_2, C_3, C_4, C_5$ , and  $C_6$  are some constants. This implies that  $f(\theta)$ ,  $f(\theta + \delta)$ , and  $f(\theta - \delta)$  in MeCAM all converge at a rate of  $O(\frac{\log T}{\sqrt{T}})$  for non-convex stochastic optimization, aligning our MeCAM with the convergence rate of first-order gradient methods, such as Adam.

As the third term in Eq. (7) is a meta-like objective function, we further approximate our MeCAM as a meta-driven approach. We perform perturbations on  $\mathcal{D}$  to generate  $\hat{\mathcal{D}}$ , a virtual meta-test set. In this study, we apply Mixstyle [85] for perturbations. We then derive an approximation for the third term in Eq. (7).

**Proposition 3.5.** *When the perturbation  $\delta$  is small, we*

---

**Algorithm 1: MeCAM Algorithm.**

---

**Initialize** : Initialize  $t$  and  $\theta_0$  with 0 and initial parameters, respectively.

**Input:** Training set  $\mathcal{D}$ , batch size  $b$ , learning rate  $\eta_t$ , perturbation radius  $\rho_t$ , hyperparameters  $\alpha$  and  $\beta$ , small constant  $\epsilon$ , and total number of iterations  $T$

- 1: **for**  $t$  **to**  $T$  **do**
- 2:   Sample mini-batch data  $\mathcal{B}$  from  $\mathcal{D}$ ;
- 3:   Forward  $f(\theta_t)$  on  $\mathcal{B}$  and then back-propagate the gradients;
- 4:   Compute the perturbation  $\delta_t = \rho_t \frac{\nabla f(\theta_t)}{\|\nabla f(\theta_t)\| + \epsilon}$ ;
- 5:   Forward  $f(\theta_t + \delta_t)$  on  $\mathcal{B}$  and then back-propagate the gradients;
- 6:   Forward  $m(\theta_t - \delta_t)$  on  $\tilde{\mathcal{B}}$  obtained by utilizing Mixstyle and then back-propagate the gradients;
- 7:   Update:  $\theta_{t+1} \leftarrow \theta_t - \eta_t((1 - \alpha - \beta)\nabla f(\theta_t) + \alpha\nabla f(\theta_t + \delta_t) + \beta\nabla m(\theta_t - \delta_t))$
- 8: **end for**

**Output:**  $\theta_t$

---

have

$$\alpha(f(\theta - \delta) - f(\theta)) \approx \beta(m(\theta - \delta) - f(\theta)), \quad (10)$$

where  $\beta$  is another hyperparameter balancing the terms, with the condition of  $\beta \leq \alpha$ . The proof can be found in Supplementary Material A. Since we denote  $f(\theta; \mathcal{D})$  as  $f(\theta)$ , we utilize  $m(\theta - \delta)$  to represent  $f(\theta - \delta; \tilde{\mathcal{D}})$  for clarity.  $m(\theta - \delta)$  is designed to emulate the deployment environment to assess the model when transferred from the training set  $\mathcal{D}$  to the virtual meta-test set  $\tilde{\mathcal{D}}$ , indicating the robustness of the current model across different data distributions. Finally, by combining both Eq. (7) and Eq. (10), the overall objective of MeCAM is:

$$\min_{\theta} f(\theta) + \underbrace{\alpha(f(\theta + \delta) - f(\theta))}_{\text{surrogate gap of SAM}} + \underbrace{\beta(m(\theta - \delta) - f(\theta))}_{\text{surrogate gap of meta-learning}}, \quad (11)$$

where the second and third terms in the right side can be regarded as the surrogate gap of SAM and the surrogate gap of meta-learning, respectively. A smaller gap between the loss of SAM (*i.e.*,  $f(\theta + \delta)$ ) or meta-learning (*i.e.*,  $m(\theta - \delta)$ ) and the vanilla training loss (*i.e.*,  $f(\theta)$ ) indicates a flatter loss landscape, which contributes to the robustness of the model. Previous work [75, 89] has also demonstrated the superiority of the surrogate gap over the vanilla training loss. Compared to directly calculating the Hessian, the process in our MeCAM is much easier and less computational, allowing our method to be used like other conventional optimizers, such as Adam [32]. The optimization procedure of MeCAM is outlined in Algorithm 1.

Table 1. The dataset details of PACS, VLCS, OfficeHome, TerraIncognita, and DomainNet.

Dataset	Domains	Images	Classes
PACS [38]	4	9,991	7
VLCS [17]	4	10,729	5
OfficeHome [71]	4	15,588	65
TerraIncognita [6]	4	24,788	10
DomainNet [57]	6	586,575	345

## 4. Experiments

### 4.1. Datasets and Implementation Details

We evaluated our MeCAM against other competing methods on five public DG benchmarks, including PACS [38], VLCS [17], OfficeHome [71], TerraIncognita [6], and DomainNet [57]. The details of each dataset can be found in Table 1.

For a fair comparison, we adopted the training and evaluation protocols from DomainBed [23], where hyperparameter tuning was performed without access to test data. All models were trained on DomainNet for 15,000 iterations and on the other datasets for 5,000 iterations, unless otherwise specified. We used the leave-one-domain-out protocol for evaluation, where one domain is held out as the target (test) domain, and the remaining domains serve as the source (training) domains. For each dataset, 20% of the training data was used for validation and model selection. We utilized the average accuracy across all domains to measure the performance of each model and performed three experimental trials (*i.e.*, setting the random seed to 0, 1, and 2) to compute the mean value and standard error of the performance metric. The default backbone used in this study is the ResNet-50 [24] pretrained on ImageNet [61]. We utilized the Adam optimizer [32] as the base optimizer for MeCAM. The optimal hyperparameter settings of MeCAM for each dataset are provided in Supplementary Material B.

### 4.2. Comparison with Existing DG Methods

We compared our MeCAM with 25 existing conventional DG methods [4, 7, 8, 10, 13, 21, 26, 31, 33, 39, 40, 43, 52, 62, 64, 66, 67, 70, 77, 81, 85] to evaluate its generalization ability. The results were presented in Table 2. Compared to the ERM algorithm [70], which can be treated as the baseline, MeCAM consistently demonstrates a substantial improvement across all benchmarks, with an average performance gain of 2.7%. MeCAM outperforms most methods on all datasets, with particularly notable improvements on PACS, VLCS, and DomainNet. Specifically, MeCAM achieves a 1.8% improvement over MADG on PACS, a 1.1% improvement over GMDG on VLCS, and a 0.4% improvement over GMDG on DomainNet. Although

Table 2. Average accuracy and standard error ( $mean_{\pm std}$ ) of our MeCAM and existing DG methods calculated across three trials on five public DG datasets. The best results are highlighted in **bold**. The results denoted by † are taken from [75] and [13], while the results marked by ‡ are obtained directly from the original source.

Algorithm	PACS	VLCS	OfficeHome	TerraInc	DomainNet	Average
MMD† [40]	84.7 $\pm$ 0.5	77.5 $\pm$ 0.9	66.3 $\pm$ 0.1	42.2 $\pm$ 1.6	23.4 $\pm$ 9.5	58.8
Mixstyle† [85]	85.2 $\pm$ 0.3	77.9 $\pm$ 0.5	60.4 $\pm$ 0.3	44.0 $\pm$ 0.7	34.0 $\pm$ 0.1	60.3
GroupDRO† [62]	84.4 $\pm$ 0.8	76.7 $\pm$ 0.6	66.0 $\pm$ 0.7	43.2 $\pm$ 1.1	33.3 $\pm$ 0.2	60.7
IRM† [4]	83.5 $\pm$ 0.8	78.5 $\pm$ 0.5	64.3 $\pm$ 2.2	47.6 $\pm$ 0.8	33.9 $\pm$ 2.8	61.6
ARM† [81]	85.1 $\pm$ 0.4	77.6 $\pm$ 0.3	64.8 $\pm$ 0.3	45.5 $\pm$ 0.3	35.5 $\pm$ 0.2	61.7
VREx† [33]	84.9 $\pm$ 0.6	78.3 $\pm$ 0.2	66.4 $\pm$ 0.6	46.4 $\pm$ 0.6	33.6 $\pm$ 2.9	61.9
AND-mask† [56]	86.4 $\pm$ 0.4	76.4 $\pm$ 0.4	66.1 $\pm$ 0.2	49.8 $\pm$ 0.4	37.9 $\pm$ 0.6	63.3
CDANN† [43]	82.6 $\pm$ 0.9	77.5 $\pm$ 0.1	65.8 $\pm$ 1.3	45.8 $\pm$ 1.6	38.3 $\pm$ 0.3	62.0
SAND-mask‡ [64]	84.4 $\pm$ 0.9	78.1 $\pm$ 0.9	65.6 $\pm$ 0.4	44.6 $\pm$ 0.3	37.2 $\pm$ 0.6	62.0
DANN† [21]	83.6 $\pm$ 0.4	78.6 $\pm$ 0.4	65.9 $\pm$ 0.6	46.7 $\pm$ 0.5	38.3 $\pm$ 0.1	62.6
RSC† [26]	85.2 $\pm$ 0.9	77.1 $\pm$ 0.5	65.5 $\pm$ 0.9	46.6 $\pm$ 1.0	38.9 $\pm$ 0.5	62.7
MTL† [7]	84.6 $\pm$ 0.5	77.2 $\pm$ 0.4	66.4 $\pm$ 0.5	45.6 $\pm$ 1.2	40.6 $\pm$ 0.1	62.9
Mixup† [77]	84.6 $\pm$ 0.6	77.4 $\pm$ 0.6	68.1 $\pm$ 0.3	47.9 $\pm$ 0.8	39.2 $\pm$ 0.1	63.4
MLDG† [39]	84.9 $\pm$ 1.0	77.2 $\pm$ 0.4	66.8 $\pm$ 0.6	47.7 $\pm$ 0.9	41.2 $\pm$ 0.1	63.6
ERM† [70]	85.5 $\pm$ 0.2	77.3 $\pm$ 0.4	66.5 $\pm$ 0.3	46.1 $\pm$ 1.8	43.8 $\pm$ 0.1	63.9
Fish‡ [66]	85.5 $\pm$ 0.3	77.8 $\pm$ 0.3	68.6 $\pm$ 0.4	45.1 $\pm$ 1.3	42.7 $\pm$ 0.2	63.9
SagNet† [52]	86.3 $\pm$ 0.2	77.8 $\pm$ 0.5	68.1 $\pm$ 0.1	48.6 $\pm$ 1.0	40.3 $\pm$ 0.1	64.2
SelfReg‡ [31]	85.6 $\pm$ 0.4	77.8 $\pm$ 0.9	67.9 $\pm$ 0.7	47.0 $\pm$ 0.3	42.8 $\pm$ 0.0	64.2
CORAL† [67]	86.2 $\pm$ 0.3	78.8 $\pm$ 0.6	68.7 $\pm$ 0.3	47.6 $\pm$ 1.0	41.5 $\pm$ 0.1	64.5
mDSDI‡ [8]	86.2 $\pm$ 0.2	79.0 $\pm$ 0.3	69.2 $\pm$ 0.4	48.1 $\pm$ 1.4	42.8 $\pm$ 0.1	65.1
Fishr† [60]	86.9 $\pm$ 0.2	78.2 $\pm$ 0.2	68.2 $\pm$ 0.2	53.6 $\pm$ 0.4	41.8 $\pm$ 0.2	65.7
MIRO‡ [10]	85.4 $\pm$ 0.4	79.0 $\pm$ 0.0	70.5 $\pm$ 0.4	50.4 $\pm$ 1.1	44.3 $\pm$ 0.2	65.9
LP-FT‡ [34]	84.6 $\pm$ 0.8	76.7 $\pm$ 1.5	65.0 $\pm$ 0.2	47.1 $\pm$ 0.7	43.0 $\pm$ 0.1	63.3
MADG† [13]	86.5 $\pm$ 0.4	78.7 $\pm$ 0.2	<b>71.3</b> $\pm$ 0.3	<b>53.7</b> $\pm$ 0.5	39.9 $\pm$ 0.4	66.0
GMDG‡ [69]	85.6 $\pm$ 0.3	79.2 $\pm$ 0.3	70.7 $\pm$ 0.2	51.1 $\pm$ 0.9	44.6 $\pm$ 0.1	66.3
MeCAM (Ours)	<b>88.3</b> $\pm$ 0.3	<b>80.3</b> $\pm$ 0.3	70.4 $\pm$ 0.4	48.9 $\pm$ 1.1	<b>45.0</b> $\pm$ 0.0	<b>66.6</b>

MADG achieves the highest performance on OfficeHome and TerraIncognita, its performance on DomainNet is relatively weak. DomainNet is the largest dataset with over half a million images across 345 categories and collected from six distinct domains, posing a significant challenge. Our MeCAM surpasses other DG methods on this dataset, highlighting its robustness in handling such a large-scale and complex dataset. Overall, these results demonstrate that MeCAM improves the model generalization across a wide range of DG tasks.

### 4.3. Comparison with Optimizers and Sharpness-Based DG Methods

Since MeCAM can be viewed as an optimizer designed to improve the update of model parameter, we further compared it with six other optimizers and six sharpness-based DG methods from the perspective of model optimization. The results were shown in Table 3. It reveals that: (1) AdaHessian achieves the best overall performance among

the optimizers, indicating the effectiveness of Hessian-based optimization for enhancing generalization; (2) even the sharpness-based method with the lowest performance, *i.e.*, SAM, outperforms all the optimizers, demonstrating the importance of reducing sharpness of the loss landscape for better generalization; (3) different datasets exhibit preferences for different algorithms, *e.g.*, AdaHessian outperforms AdamW on PACS, VLCS, and DomainNet, but possesses lower performance on OfficeHome and DomainNet; and (4) MeCAM consistently outperforms other optimizers and sharpness-based methods across all benchmark datasets, confirming that simultaneously minimizing the surrogate gap of SAM and meta-learning for reducing curvature around the local minima leads to superior generalization.

### 4.4. Ablation Study

To better understand the contributions of each component in MeCAM, we conducted an ablation study on the three

Table 3. Average accuracy and standard error ( $mean_{\pm std}$ ) of our MeCAM, optimizers, and existing sharpness-based DG methods calculated across three trials on five DG datasets. The best results are highlighted in **bold**. Results marked with † and ‡ are taken from [75] and the original source, respectively.

Algorithm		PACS	VLCS	OfficeHome	TerraInc	DomainNet	Average
Optimizer	Adam† [32]	84.2±0.6	77.3±1.3	67.6±0.4	44.4±0.8	43.0±0.1	63.3
	AdamW† [47]	83.6±1.5	77.4±0.8	68.8±0.6	45.2±1.4	43.4±0.1	63.7
	SGD† [53]	79.9±1.4	78.1±0.2	68.5±0.3	44.9±1.8	43.2±0.1	62.9
	YOGI† [80]	81.2±0.4	77.6±0.6	68.3±0.3	45.4±0.5	43.5±0.0	63.2
	AdaBelief† [88]	84.6±0.6	78.4±0.4	68.0±0.9	45.2±2.0	43.5±0.1	63.9
	AdaHessian† [79]	84.5±1.0	78.6±0.8	68.4±0.9	44.4±0.5	44.4±0.1	64.1
Sharpness-based	SAM† [20]	85.3±1.0	78.2±0.5	68.0±0.8	45.7±0.9	43.4±0.1	64.1
	GAM† [83]	86.1±0.6	78.5±0.4	68.2±1.0	45.2±0.6	43.8±0.1	64.4
	SAGM* [75]	86.9±0.3	79.1±1.0	69.4±0.1	48.6±1.5	44.7±0.2	65.7
	FAD† [82]	88.2±0.5	78.9±0.8	69.2±0.5	45.7±1.0	44.4±0.1	65.3
	CRSAM* [76]	85.4±0.7	79.1±0.6	68.9±1.0	45.3±0.4	44.3±0.1	64.6
	FSAM* [42]	86.5±0.3	79.4±0.1	70.2±0.1	46.1±0.6	44.9±0.1	65.4
MeCAM (Ours)		<b>88.3</b> ±0.3	<b>80.3</b> ±0.3	<b>70.4</b> ±0.4	<b>48.9</b> ±1.1	<b>45.0</b> ±0.0	<b>66.6</b>

Table 4. Ablation study on various combinations of optimization objectives in our MeCAM. Average accuracy and standard error ( $mean_{\pm std}$ ) of our MeCAM and other variants are calculated across three trials on PACS, VLCS, and OfficeHome. The best results are highlighted in **bold**.

$f(\theta)$	$\alpha(f(\theta + \delta) - f(\theta))$	$\beta(m(\theta - \delta) - f(\theta))$	PACS	VLCS	OfficeHome	Average
✓			85.0±0.5	78.2±0.5	67.8±0.2	77.0
	✓		15.4±0.3	47.0±0.3	1.6±0.1	21.3
		✓	46.1±5.2	44.2±2.9	2.3±0.2	30.9
✓	✓		86.4±1.3	<b>80.3</b> ±0.5	69.7±0.2	78.8
✓		✓	86.7±0.5	79.7±0.3	69.5±0.5	78.6
	✓	✓	87.4±0.1	79.4±0.1	69.8±0.2	78.9
✓	✓	✓	<b>88.3</b> ±0.3	<b>80.3</b> ±0.3	<b>70.4</b> ±0.4	<b>79.7</b>

terms of MeCAM’s optimization objective (see Eq. (11)). The results were displayed in Table 4. Please note that when only  $\alpha(f(\theta + \delta) - f(\theta))$  or  $\beta(m(\theta - \delta) - f(\theta))$  is used as the optimization objective, we set  $\alpha$  or  $\beta$  to 1. The results highlight the following insights: (1) using only  $f(\theta)$  degenerates MeCAM to ERM, which does not effectively reduce sharpness or curvature; (2) relying solely on the surrogate gap of SAM or meta-learning results in significant performance degradation, particularly on the OfficeHome dataset, indicating that minimizing sharpness alone is insufficient; (3) combining the surrogate gaps of SAM or meta-learning with  $f(\theta)$  alleviates this degradation and improves generalization performance; and (4) the best performance is achieved when all three terms are jointly used in the optimization objective, suggesting the effectiveness of MeCAM. Furthermore, it is worth noting that combining the surrogate gap of SAM with meta-learning not only resolves the degradation observed when using either of them individually, but also outperforms the use of  $f(\theta)$  alone. We argue that the optimization objectives of these two terms are complementary, and their combination effectively mitigates limitations of each other.

#### 4.5. Evaluation on Various Training Iterations

To explore how the training iteration takes effect on our MeCAM and other sharpness-based methods, we further evaluated them on various training iterations using each domain of PACS as the target domain. The results were displayed in Figure 3. It shows that MeCAM outperforms other competing methods in most scenarios, particularly in the target domains of “Art painting”, “Cartoon”, and “Sketch”. On the “Photo” domain, it is hard to distinguish which method is superior over others, as performing classification on this domain is relatively simple, where all methods exhibit an accuracy over 95%. Additionally, MeCAM achieves the best overall performance across all training iterations, demonstrating its superior generalization ability and robustness.

#### 4.6. Curvature Comparison on PACS

In this experiment, we evaluated the curvature metric  $\mathcal{C}$  around the local minima obtained by our MeCAM and other competing methods. Based on the above approximation, we utilized various values of  $\rho$  to compute  $\mathcal{C}$  on the PACS dataset by  $\mathcal{C}(f(\theta)) = \alpha \frac{f(\theta+\delta) + f(\theta-\delta) - 2f(\theta)}{\|\nabla f(\theta)\|^2 + 1}$ , where  $\alpha$  is

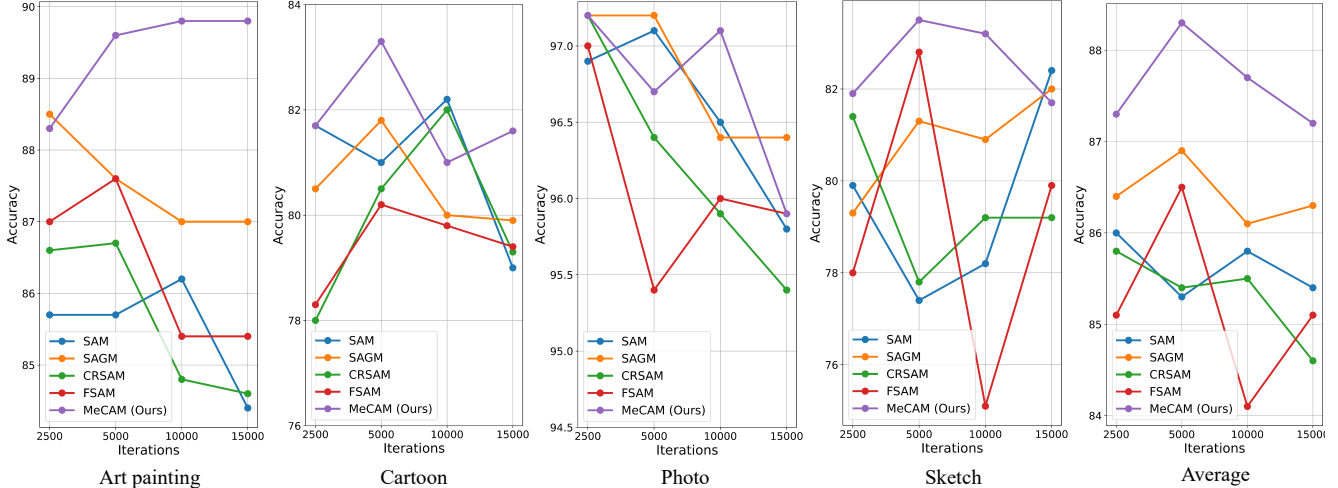


Figure 3. Accuracy of our MeCAM and other sharpness-based methods across various training iterations using each domain of PACS as the target domain. For each figure, the X-axis denotes the training iterations, where 5,000 is the default configuration, and the Y-axis indicates the accuracy.

omitted for convenient comparison. The results were listed in Table 5, with smaller curvature indicating superior algorithm. It can be found that our MeCAM consistently outperforms other competing methods across most values of  $\rho$  and improves  $\mathcal{C}$  significantly as  $\rho$  increases, demonstrating the robustness of our MeCAM against large perturbations.

Table 5. Curvature metric of our MeCAM and five competing methods on the PACS dataset with various values of  $\rho$ . The best result of each column is highlighted in **bold**.

Algorithm	$\rho = 0.01$	$\rho = 0.05$	$\rho = 0.1$	$\rho = 0.2$	$\rho = 0.5$
ERM [70]	$8.7e^{-5}$	$2.4e^{-3}$	$6.3e^{-3}$	$3.2e^{-2}$	$5.1e^{-1}$
SAM [20]	$3.8e^{-5}$	$5.4e^{-4}$	$1.9e^{-3}$	$1.9e^{-2}$	$1.8e^{-1}$
SAGM [75]	$2.9e^{-5}$	$7.6e^{-4}$	$3.3e^{-3}$	$5.2e^{-3}$	$1.1e^{-1}$
CRSAM [76]	$3.0e^{-5}$	$5.3e^{-4}$	$1.6e^{-3}$	$6.7e^{-3}$	$1.0e^{-1}$
FSAM [42]	<b><math>2.6e^{-5}</math></b>	$4.4e^{-4}$	$1.3e^{-3}$	$5.1e^{-3}$	$6.1e^{-2}$
MeCAM (Ours)	$2.8e^{-5}$	<b><math>4.2e^{-4}</math></b>	<b><math>1.1e^{-3}</math></b>	<b><math>3.2e^{-3}</math></b>	<b><math>4.4e^{-2}</math></b>

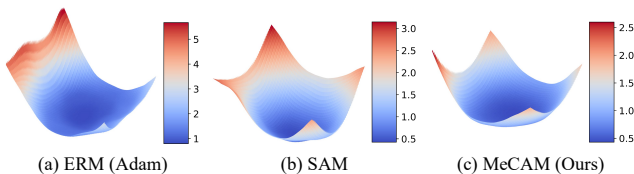


Figure 4. Visualization of the loss landscapes of ERM, SAM, and our MeCAM on the PACS dataset. The number represents the loss value.

#### 4.7. Visualization of Loss Landscapes

To demonstrate that MeCAM achieves a flatter minima, we visualized the loss landscapes of the ResNet50 trained using ERM (Adam), SAM, and our MeCAM on the PACS dataset

with 5,000 iterations. We utilized the visualization techniques proposed in [41] and plotted the loss values along two randomly sampled orthogonal Gaussian perturbations around the local minima. As shown in Figure 4, the results reveal that (1) ERM is very sensitive to perturbations; (2) our MeCAM converges to a flatter minima compared to both ERM and SAM; and (3) our MeCAM also results in a flat minima with lower loss values. These results demonstrate the superiority of MeCAM in decreasing the sharpness around the local minima.

## 5. Conclusion

In this paper, to tackle the limitations in SAM and its existing variants, we introduce a more rational training process for sharpness-based methods, incorporating a curvature metric that can better measure the sharpness. This metric focuses on the curvature around the local minima and can bound the maximum eigenvalue of the Hessian matrix. We propose a novel generalization approach, MeCAM, which minimizes both the surrogate gap of sharpness-aware minimization and the surrogate gap of meta-learning to seek a flatter minima. We demonstrate that MeCAM effectively controls the generalization error and achieves a competitive convergence rate. Compared to existing conventional DG methods and sharpness-based methods, MeCAM shows superior generalization performance across various DG datasets. In our future work, we plan to improve MeCAM by: (1) developing better methods for computing the step-size in the central difference approximation; and (2) exploring the combination of MeCAM with other meta-learning paradigms or investigating other ways to synthesize the virtual meta-test domain.



## References

- [1] Mahbubul Alam, Manar D Samad, Lasitha Vidyaratne, Alexander Glandon, and Khan M Iftekharuddin. Survey on deep neural networks in speech and vision systems. *Neuro-computing*, 417:302–321, 2020. [1](#)
- [2] Md Zahangir Alom, Tarek M Taha, Chris Yakopcic, Stefan Westberg, Paheding Sidike, Mst Shamima Nasrin, Mahmudul Hasan, Brian C Van Essen, Abdul AS Awwal, and Vijayan K Asari. A state-of-the-art survey on deep learning theory and architectures. *electronics*, 8(3):292, 2019. [1](#)
- [3] Maksym Andriushchenko and Nicolas Flammarion. Towards understanding sharpness-aware minimization. In *Int. Conf. Mach. Learn.*, pages 639–668. PMLR, 2022. [2](#)
- [4] Martin Arjovsky, Léon Bottou, Ishaan Gulrajani, and David Lopez-Paz. Invariant risk minimization. *arXiv preprint arXiv:1907.02893*, 2019. [5](#), [6](#), [4](#), [7](#), [8](#), [9](#)
- [5] Yogesh Balaji, Swami Sankaranarayanan, and Rama Chellappa. Metareg: Towards domain generalization using meta-regularization. *Advances in neural information processing systems*, 31, 2018. [3](#)
- [6] Sara Beery, Grant Van Horn, and Pietro Perona. Recognition in terra incognita. In *ECCV*, pages 456–473, 2018. [5](#)
- [7] Gilles Blanchard, Aniket Anand Deshmukh, Urun Dogan, Gyemin Lee, and Clayton Scott. Domain generalization by marginal transfer learning. *Journal of machine learning research*, 22(2):1–55, 2021. [5](#), [6](#), [4](#), [7](#), [8](#), [9](#)
- [8] Manh-Ha Bui, Toan Tran, Anh Tran, and Dinh Phung. Exploiting domain-specific features to enhance domain generalization. *NeurIPS*, 34:21189–21201, 2021. [5](#), [6](#)
- [9] Junbum Cha, Sanghyuk Chun, Kyungjae Lee, Han-Cheol Cho, Seunghyun Park, Yunsung Lee, and Sungrae Park. Swad: Domain generalization by seeking flat minima. *NeurIPS*, 34:22405–22418, 2021. [4](#)
- [10] Junbum Cha, Kyungjae Lee, Sungrae Park, and Sanghyuk Chun. Domain generalization by mutual-information regularization with pre-trained models. In *ECCV*, pages 440–457. Springer, 2022. [5](#), [6](#)
- [11] Xiangning Chen, Cho-Jui Hsieh, and Boqing Gong. When vision transformers outperform resnets without pre-training or strong data augmentations. In *ICLR*, 2022. [3](#)
- [12] Ziyang Chen, Yongsheng Pan, Yiwen Ye, Hengfei Cui, and Yong Xia. Treasure in distribution: a domain randomization based multi-source domain generalization for 2d medical image segmentation. In *Int. Conf. Med. Image Comput. Comput.-Assist. Intervent.*, pages 89–99. Springer, 2023. [2](#)
- [13] Aven Dayal, Vimal KB, Linga Reddy Cenkaramaddi, C Mohan, Abhinav Kumar, and Vineeth N Balasubramanian. Madg: margin-based adversarial learning for domain generalization. *NeurIPS*, 36, 2024. [5](#), [6](#), [4](#), [7](#), [8](#), [9](#)
- [14] John E Dennis Jr and Robert B Schnabel. *Numerical methods for unconstrained optimization and nonlinear equations*. SIAM, 1996. [4](#)
- [15] Laurent Dinh, Razvan Pascanu, Samy Bengio, and Yoshua Bengio. Sharp minima can generalize for deep nets. In *Int. Conf. Mach. Learn.*, pages 1019–1028. PMLR, 2017. [2](#)
- [16] Jiawei Du, Hanshu Yan, Jiashi Feng, Joey Tianyi Zhou, Liangli Zhen, Rick Siow Mong Goh, and Vincent Tan. Efficient sharpness-aware minimization for improved training of neural networks. In *ICLR*, 2021. [2](#)
- [17] Chen Fang, Ye Xu, and Daniel N Rockmore. Unbiased metric learning: On the utilization of multiple datasets and web images for softening bias. In *ICCV*, pages 1657–1664, 2013. [5](#)
- [18] Herbert Federer. Curvature measures. *Transactions of the American Mathematical Society*, 93(3):418–491, 1959. [3](#)
- [19] Chelsea Finn, Pieter Abbeel, and Sergey Levine. Model-agnostic meta-learning for fast adaptation of deep networks. In *Int. Conf. Mach. Learn.*, pages 1126–1135. PMLR, 2017. [2](#)
- [20] Pierre Foret, Ariel Kleiner, Hossein Mobahi, and Behnam Neyshabur. Sharpness-aware minimization for efficiently improving generalization. In *ICLR*, 2021. [1](#), [2](#), [3](#), [7](#), [8](#), [4](#), [5](#), [6](#), [9](#)
- [21] Yaroslav Ganin, Evgeniya Ustinova, Hana Ajakan, Pascal Germain, Hugo Larochelle, François Laviolette, Mario March, and Victor Lempitsky. Domain-adversarial training of neural networks. *Journal of machine learning research*, 17(59):1–35, 2016. [5](#), [6](#), [4](#), [7](#), [8](#), [9](#)
- [22] Timur Garipov, Pavel Izmailov, Dmitrii Podoprikin, Dmitry P Vetrov, and Andrew G Wilson. Loss surfaces, mode connectivity, and fast ensembling of dnns. *NeurIPS*, 31, 2018. [1](#), [2](#)
- [23] Ishaan Gulrajani and David Lopez-Paz. In search of lost domain generalization. In *ICLR*, 2021. [5](#), [4](#)
- [24] Kaiming He, Xiangyu Zhang, Shaoqing Ren, and Jian Sun. Deep residual learning for image recognition. In *CVPR*, pages 770–778, 2016. [5](#)
- [25] Sepp Hochreiter and Jürgen Schmidhuber. Simplifying neural nets by discovering flat minima. *NeurIPS*, 7, 1994. [1](#), [2](#)
- [26] Zeyi Huang, Haohan Wang, Eric P Xing, and Dong Huang. Self-challenging improves cross-domain generalization. In *ECCV*, pages 124–140. Springer, 2020. [5](#), [6](#), [4](#), [7](#), [8](#), [9](#)
- [27] Mike Huisman, Jan N Van Rijn, and Aske Plaat. A survey of deep meta-learning. *Artificial Intelligence Review*, 54(6):4483–4541, 2021. [2](#)
- [28] Simran Kaur, Jeremy Cohen, and Zachary Chase Lipton. On the maximum hessian eigenvalue and generalization. In *I Can’t Believe It’s Not Better Workshop: Understanding Deep Learning Through Empirical Falsification*, pages 51–65. PMLR, 2023. [3](#)
- [29] Nitish Shirish Keskar, Dheevatsa Mudigere, Jorge Nocedal, Mikhail Smelyanskiy, and Ping Tak Peter Tang. On large-batch training for deep learning: Generalization gap and sharp minima. In *ICLR*, 2016. [1](#), [2](#), [3](#)
- [30] Arsham Gholamzadeh Khooe, Yanan Yu, and Robert Feldt. Domain generalization through meta-learning: a survey. *Artificial Intelligence Review*, 57(10):285, 2024. [2](#)
- [31] Daehee Kim, Youngjun Yoo, Seunghyun Park, Jinkyu Kim, and Jaekoo Lee. Selfreg: Self-supervised contrastive regularization for domain generalization. In *Proceedings of the IEEE/CVF International Conference on Computer Vision*, pages 9619–9628, 2021. [5](#), [6](#)

- [32] Diederik P Kingma. Adam: A method for stochastic optimization. *arXiv preprint arXiv:1412.6980*, 2014. [5](#), [7](#), [4](#), [6](#), [8](#), [9](#)
- [33] David Krueger, Ethan Caballero, Joern-Henrik Jacobsen, Amy Zhang, Jonathan Binas, Dinghui Zhang, Remi Le Priol, and Aaron Courville. Out-of-distribution generalization via risk extrapolation (rex). In *Int. Conf. Mach. Learn.*, pages 5815–5826. PMLR, 2021. [5](#), [6](#), [4](#), [7](#), [8](#), [9](#)
- [34] Ananya Kumar, Aditi Raghunathan, Robbie Matthew Jones, Tengyu Ma, and Percy Liang. Fine-tuning can distort pre-trained features and underperform out-of-distribution. In *ICLR*, 2022. [6](#)
- [35] Jungmin Kwon, Jeongseop Kim, Hyunseo Park, and In Kwon Choi. Asam: Adaptive sharpness-aware minimization for scale-invariant learning of deep neural networks. In *ICLR*, pages 5905–5914. PMLR, 2021. [2](#)
- [36] Beatrice Laurent and Pascal Massart. Adaptive estimation of a quadratic functional by model selection. *Annals of statistics*, pages 1302–1338, 2000. [1](#)
- [37] Binh M Le and Simon S Woo. Gradient alignment for cross-domain face anti-spoofing. In *CVPR*, pages 188–199, 2024. [1](#), [2](#)
- [38] Da Li, Yongxin Yang, Yi-Zhe Song, and Timothy M Hospedales. Deeper, broader and artier domain generalization. In *ICCV*, pages 5542–5550, 2017. [5](#)
- [39] Da Li, Yongxin Yang, Yi-Zhe Song, and Timothy Hospedales. Learning to generalize: Meta-learning for domain generalization. In *AAAI*, 2018. [3](#), [5](#), [6](#), [4](#), [7](#), [8](#), [9](#)
- [40] Haoliang Li, Sinno Jialin Pan, Shiqi Wang, and Alex C Kot. Domain generalization with adversarial feature learning. In *CVPR*, pages 5400–5409, 2018. [5](#), [6](#), [4](#), [7](#), [8](#), [9](#)
- [41] Hao Li, Zheng Xu, Gavin Taylor, Christoph Studer, and Tom Goldstein. Visualizing the loss landscape of neural nets. *NeurIPS*, 31, 2018. [8](#)
- [42] Tao Li, Pan Zhou, Zhengbao He, Xinwen Cheng, and Xiaolin Huang. Friendly sharpness-aware minimization. In *CVPR*, pages 5631–5640, 2024. [1](#), [7](#), [8](#), [4](#), [5](#), [6](#), [9](#)
- [43] Ya Li, Mingming Gong, Xinmei Tian, Tongliang Liu, and Dacheng Tao. Domain generalization via conditional invariant representations. In *AAAI*, 2018. [5](#), [6](#), [4](#), [7](#), [8](#), [9](#)
- [44] Ya Li, Xinmei Tian, Mingming Gong, Yajing Liu, Tongliang Liu, Kun Zhang, and Dacheng Tao. Deep domain generalization via conditional invariant adversarial networks. In *ECCV*, pages 624–639, 2018. [2](#)
- [45] Quande Liu, Qi Dou, Lequan Yu, and Pheng Ann Heng. Msnet: multi-site network for improving prostate segmentation with heterogeneous mri data. *IEEE Trans. Med. Imaging*, 39(9):2713–2724, 2020. [1](#), [2](#)
- [46] Yong Liu, Siqi Mai, Xiangning Chen, Cho-Jui Hsieh, and Yang You. Towards efficient and scalable sharpness-aware minimization. In *CVPR*, pages 12360–12370, 2022. [2](#)
- [47] I Loshchilov. Decoupled weight decay regularization. *arXiv preprint arXiv:1711.05101*, 2017. [7](#), [4](#), [5](#), [6](#), [8](#), [9](#)
- [48] David A McAllester. Pac-bayesian model averaging. In *Proceedings of the twelfth annual conference on Computational learning theory*, pages 164–170, 1999. [4](#)
- [49] Sparsh Mittal. A survey on modeling and improving reliability of dnn algorithms and accelerators. *Journal of Systems Architecture*, 104:101689, 2020. [1](#)
- [50] Krikamol Muandet, David Balduzzi, and Bernhard Schölkopf. Domain generalization via invariant feature representation. In *Int. Conf. Mach. Learn.*, pages 10–18. PMLR, 2013. [1](#), [2](#)
- [51] Usman Muhammad, Jorma Laaksonen, Djamila Romaiisa Beddiar, and Mourad Oussalah. Domain generalization via ensemble stacking for face presentation attack detection. *IJCV*, pages 1–24, 2024. [2](#)
- [52] Hyeonseob Nam, HyunJae Lee, Jongchan Park, Wonjun Yoon, and Donggeun Yoo. Reducing domain gap by reducing style bias. In *CVPR*, pages 8690–8699, 2021. [5](#), [6](#), [4](#), [7](#), [8](#), [9](#)
- [53] Yurii Nesterov. A method for solving the convex programming problem with convergence rate  $o(1/k^2)$ . In *Dokl akad nauk Ssr*, page 543, 1983. [7](#), [4](#), [5](#), [6](#), [8](#), [9](#)
- [54] Li Niu, Wen Li, and Dong Xu. Multi-view domain generalization for visual recognition. In *ICCV*, pages 4193–4201, 2015. [1](#), [2](#)
- [55] Jorge Nocedal and Stephen J Wright. *Numerical optimization*. Springer, 1999. [4](#)
- [56] Giambattista Parascandolo, Alexander Neitz, Antonio Orvieto, Luigi Gresele, and Bernhard Schölkopf. Learning explanations that are hard to vary. In *ICLR*. OpenReview, 2021. [6](#), [4](#), [5](#), [7](#), [8](#), [9](#)
- [57] Xingchao Peng, Qinxun Bai, Xide Xia, Zijun Huang, Kate Saenko, and Bo Wang. Moment matching for multi-source domain adaptation. In *Proceedings of the IEEE/CVF international conference on computer vision*, pages 1406–1415, 2019. [5](#)
- [58] Xingchao Peng, Zijun Huang, Ximeng Sun, and Kate Saenko. Domain agnostic learning with disentangled representations. In *Int. Conf. Mach. Learn.*, pages 5102–5112. PMLR, 2019. [1](#), [2](#)
- [59] Vihari Piratla, Praneeth Netrapalli, and Sunita Sarawagi. Efficient domain generalization via common-specific low-rank decomposition. In *Int. Conf. Mach. Learn.*, pages 7728–7738. PMLR, 2020. [2](#)
- [60] Alexandre Rame, Corentin Dancette, and Matthieu Cord. Fishr: Invariant gradient variances for out-of-distribution generalization. In *Int. Conf. Mach. Learn.*, pages 18347–18377. PMLR, 2022. [6](#), [4](#), [5](#), [7](#), [8](#), [9](#)
- [61] Olga Russakovsky, Jia Deng, Hao Su, Jonathan Krause, Sanjeev Satheesh, Sean Ma, Zhiheng Huang, Andrej Karpathy, Aditya Khosla, Michael Bernstein, et al. Imagenet large scale visual recognition challenge. *IJCV*, 115:211–252, 2015. [5](#)
- [62] Shiori Sagawa, Pang Wei Koh, Tatsunori B Hashimoto, and Percy Liang. Distributionally robust neural networks. In *ICLR*, 2019. [5](#), [6](#), [4](#), [7](#), [8](#), [9](#)
- [63] Swami Sankaranarayanan, Yogesh Balaji, Arpit Jain, Ser Nam Lim, and Rama Chellappa. Learning from synthetic data: Addressing domain shift for semantic segmentation. In *CVPR*, pages 3752–3761, 2018. [1](#)

- [64] Soroosh Shahtalebi, Jean-Christophe Gagnon-Audet, Touraj Laleh, Mojtaba Faramarzi, Kartik Ahuja, and Irina Rish. Sand-mask: An enhanced gradient masking strategy for the discovery of invariances in domain generalization. *arXiv preprint arXiv:2106.02266*, 2021. 5, 6
- [65] Rui Shao, Xiangyuan Lan, Jiawei Li, and Pong C Yuen. Multi-adversarial discriminative deep domain generalization for face presentation attack detection. In *CVPR*, pages 10023–10031, 2019. 2
- [66] Yuge Shi, Jeffrey Seely, Philip Torr, N Siddharth, Awni Hannun, Nicolas Usunier, and Gabriel Synnaeve. Gradient matching for domain generalization. In *ICLR*, 2021. 5, 6
- [67] Baochen Sun and Kate Saenko. Deep coral: Correlation alignment for deep domain adaptation. In *ECCV*, pages 443–450. Springer, 2016. 5, 6, 4, 7, 8, 9
- [68] Yiyu Sun, Yaojie Liu, Xiaoming Liu, Yixuan Li, and Wen-Sheng Chu. Rethinking domain generalization for face anti-spoofing: Separability and alignment. In *CVPR*, pages 24563–24574, 2023. 2
- [69] Zhaorui Tan, Xi Yang, and Kaizhu Huang. Rethinking multi-domain generalization with a general learning objective. In *Proceedings of the IEEE/CVF Conference on Computer Vision and Pattern Recognition*, pages 23512–23522, 2024. 6, 4, 5, 7, 8, 9
- [70] Vladimir Vapnik. Statistical learning theory. *NY: Wiley*, 2: 831–842, 1998. 5, 6, 8, 4, 7, 9
- [71] Hemanth Venkateswara, Jose Eusebio, Shayok Chakraborty, and Sethuraman Panchanathan. Deep hashing network for unsupervised domain adaptation. In *CVPR*, pages 5018–5027, 2017. 5
- [72] Guoqing Wang, Hu Han, Shiguang Shan, and Xilin Chen. Cross-domain face presentation attack detection via multi-domain disentangled representation learning. In *CVPR*, pages 6678–6687, 2020. 1, 2
- [73] Jindong Wang, Cuiling Lan, Chang Liu, Yidong Ouyang, Tao Qin, Wang Lu, Yiqiang Chen, Wenjun Zeng, and S Yu Philip. Generalizing to unseen domains: A survey on domain generalization. *IEEE Trans. Knowledge Data Eng.*, 35 (8):8052–8072, 2022. 2
- [74] Mengzhu Wang, Yuehua Liu, Jianlong Yuan, Shanshan Wang, Zhibin Wang, and Wei Wang. Inter-class and inter-domain semantic augmentation for domain generalization. *IEEE TIP*, 2024. 1, 2
- [75] Pengfei Wang, Zhaoxiang Zhang, Zhen Lei, and Lei Zhang. Sharpness-aware gradient matching for domain generalization. In *CVPR*, pages 3769–3778, 2023. 1, 2, 3, 5, 6, 7, 8, 4, 9
- [76] Tao Wu, Tie Luo, and Donald C Wunsch II. CR-SAM: Curvature regularized sharpness-aware minimization. In *AAAI*, pages 6144–6152, 2024. 1, 2, 7, 8, 4, 5, 6, 9
- [77] Minghao Xu, Jian Zhang, Bingbing Ni, Teng Li, Chengjie Wang, Qi Tian, and Wenjun Zhang. Adversarial domain adaptation with domain mixup. In *AAAI*, pages 6502–6509, 2020. 5, 6, 4, 7, 8, 9
- [78] Zhewei Yao, Amir Gholami, Kurt Keutzer, and Michael W Mahoney. Pyhessian: Neural networks through the lens of the hessian. In *2020 IEEE international conference on big data (Big data)*, pages 581–590. IEEE, 2020. 3
- [79] Zhewei Yao, Amir Gholami, Sheng Shen, Mustafa Mustafa, Kurt Keutzer, and Michael Mahoney. Adahessian: An adaptive second order optimizer for machine learning. In *AAAI*, pages 10665–10673, 2021. 7, 4, 5, 6, 8, 9
- [80] Manzil Zaheer, Sashank Reddi, Devendra Sachan, Satyen Kale, and Sanjiv Kumar. Adaptive methods for nonconvex optimization. *NeurIPS*, 31, 2018. 7, 4, 5, 6, 8, 9
- [81] Marvin Zhang, Henrik Marklund, Abhishek Gupta, Sergey Levine, and Chelsea Finn. Adaptive risk minimization: A meta-learning approach for tackling group shift. *arXiv preprint arXiv:2007.02931*, 8(9), 2020. 5, 6, 4, 7, 8, 9
- [82] Xingxuan Zhang, Renzhe Xu, Han Yu, Yancheng Dong, Pengfei Tian, and Peng Cui. Flatness-aware minimization for domain generalization. In *Proceedings of the IEEE/CVF International Conference on Computer Vision*, pages 5189–5202, 2023. 7, 4, 5, 6, 8, 9, 10
- [83] Xingxuan Zhang, Renzhe Xu, Han Yu, Hao Zou, and Peng Cui. Gradient norm aware minimization seeks first-order flatness and improves generalization. In *CVPR*, pages 20247–20257, 2023. 2, 3, 7, 1, 4, 5, 6, 8, 9
- [84] Kaiyang Zhou, Yongxin Yang, Timothy Hospedales, and Tao Xiang. Learning to generate novel domains for domain generalization. In *ECCV*, pages 561–578. Springer, 2020. 1, 2
- [85] Kaiyang Zhou, Yongxin Yang, Yu Qiao, and Tao Xiang. Domain generalization with mixstyle. In *ICLR*, 2021. 2, 4, 5, 6, 7, 8, 9
- [86] Kaiyang Zhou, Yongxin Yang, Yu Qiao, and Tao Xiang. Domain adaptive ensemble learning. *IEEE TIP*, 30:8008–8018, 2021. 2
- [87] Kaiyang Zhou, Ziwei Liu, Yu Qiao, Tao Xiang, and Chen Change Loy. Domain generalization: A survey. *IEEE TPAMI*, 45(4):4396–4415, 2022. 2
- [88] Juntang Zhuang, Tommy Tang, Yifan Ding, Sekhar C Tatikonda, Nicha Dvornek, Xenophon Papademetris, and James Duncan. Adabelief optimizer: Adapting stepsizes by the belief in observed gradients. *NeurIPS*, 33:18795–18806, 2020. 7, 4, 5, 6, 8, 9
- [89] Juntang Zhuang, Boqing Gong, Liangzhe Yuan, Yin Cui, Hartwig Adam, Nicha C Dvornek, James s Duncan, Ting Liu, et al. Surrogate gap minimization improves sharpness-aware training. In *ICLR*, 2022. 1, 2, 3, 5

# Meta Curvature-Aware Minimization for Domain Generalization

## Supplementary Material

In the supplementary material, we provide more details about the proofs omitted in the manuscript (Section A), the optimal hyperparameter configurations for MeCAM on each dataset (Section B), the full results of Table 2 and Table 3 in the manuscript (Section C), and additional experiments (Section D).

### A. Proofs

#### A.1. Proof of Lemma 3.1

*Proof.* Since  $\|\mathcal{C}(f(\theta))\|$  is sub-multiplicative, we have:

$$\begin{aligned} \|\mathcal{C}(f(\theta))\| &\leq \frac{\|H(\theta)\|}{\|\|\nabla f(\theta)\|^2 + 1\|} \\ &= \frac{\lambda_{max}(H(\theta))}{\|\|\nabla f(\theta)\|^2 + 1\|} \end{aligned} \quad (12)$$

$$\lambda_{max}(H(\theta)) \geq \|\mathcal{C}(f(\theta))\| \cdot \|\|\nabla f(\theta)\|^2 + 1\|.$$

In addition,

$$\begin{aligned} \|\mathcal{C}(f(\theta))\| \cdot \|\|\nabla f(\theta)\|^2 + 1\| &\geq \|\mathcal{C}(f(\theta))(\|\nabla f(\theta)\|^2 + 1)\| \\ &= \|H(\theta)\| \\ &= \lambda_{max}(H(\theta)). \end{aligned} \quad (13)$$

Combine Eq. (12) and Eq. (13), we have:

$$\|\mathcal{C}(f(\theta))\| \cdot \|\|\nabla f(\theta)\|^2 + 1\| = \lambda_{max}(H(\theta)). \quad (14)$$

#### A.2. Proof of Proposition 3.3

*Proof.* Suppose the training set has  $n$  elements drawn i.i.d. from the true distribution, and denote the loss on the training set as  $\hat{f}(\theta)$ . Let  $\theta$  be learned from the training set with a number of  $k$ . Then following the proof of Theorem 2 in [20], with probability at least  $1 - \zeta$ , we have:

$$\begin{aligned} \mathbb{E}_{\delta_i \sim \mathcal{N}(0, \sigma^2)}[f(\theta + \delta)] &\leq \mathbb{E}_{\delta_i \sim \mathcal{N}(0, \sigma^2)}[\hat{f}(\theta + \delta)] + \\ &\sqrt{\frac{\frac{1}{4}k \log(1 + \frac{\|\theta\|^2}{k\sigma^2}) + \frac{1}{4} + \log \frac{n}{\zeta} + 2 \log(6n + 3k)}{n - 1}}. \end{aligned} \quad (15)$$

Since  $\delta_i \sim \mathcal{N}(0, \sigma^2)$ ,  $\frac{\|\delta\|^2}{\sigma^2}$  has a chi-square distribution. By Lemma 1 in [36], we have that for any  $t > 0$ :

$$P\left(\frac{\|\delta\|^2}{\sigma^2} - k \geq 2\sqrt{kt} + 2t\right) \leq \exp(-t). \quad (16)$$

By  $t = \ln \sqrt{n}$ , with probability at least  $1 - \frac{1}{\sqrt{n}}$ , we have:

$$\begin{aligned} \|\delta\|^2 &\leq \sigma^2(k + 2\sqrt{k \ln \sqrt{n}} + 2 \ln \sqrt{n}) \\ &\leq \sigma^2(\sqrt{k} + \sqrt{\ln n})^2 \leq \rho^2. \end{aligned} \quad (17)$$

According to the Taylor expansion, when  $\nabla \hat{f}(\theta)$  is approaching to the local minimum and  $\delta$  is small, we can obtain:

$$\begin{aligned} \hat{f}(\theta + \delta) &\approx \hat{f}(\theta) + \delta \nabla \hat{f}(\theta) + \frac{\delta^2}{2} \hat{H}(\theta) \\ &\leq \hat{f}(\theta) + \hat{H}(\theta) \\ &\approx \hat{f}(\theta) + \alpha(\hat{f}(\theta + \delta) + \hat{f}(\theta - \delta) - 2\hat{f}(\theta)) \end{aligned} \quad (18)$$

where  $\hat{H}(\theta)$  is the Hessian obtained on the training set. Following the proof of proposition 4.3 in [83] and combining Eq. (18), Eq. (17), and Eq. (16), we have:

$$\begin{aligned} \mathbb{E}_{\delta_i \sim \mathcal{N}(0, \sigma^2)}[f(\theta + \delta)] &\leq \hat{f}(\theta) + \\ &\alpha(\hat{f}(\theta + \delta) + \hat{f}(\theta - \delta) - 2\hat{f}(\theta)) + \frac{M}{\sqrt{n}} + \\ &\sqrt{\frac{\frac{1}{4}k \log(1 + \frac{\|\theta\|^2(1 + \sqrt{\frac{\ln n}{k}})^2)}{\rho^2} + \frac{1}{4} + \log \frac{n}{\zeta} + 2 \log(6n + 3k)}{n - 1}}, \end{aligned} \quad (19)$$

where the loss function calculated on each data is bounded by  $M$ .

#### A.3. Proof of Theorem 3.4

*Proof.* For simplicity, we utilize the SGD optimizer as the base optimizer to analyze the convergence rate of our CAM. For other optimizers, such as Adam, similar results can be derived by extending our proof. Since there are three items in  $F(\theta)$ , we first analyze each one individually and then combine the results together.

##### A.3.1 Convergence W.R.T. Function $f(\theta)$

For simplicity, the update  $d_t$  of the model parameter  $\theta$  at step  $t$  can be written as:

$$d_t = -\eta_t(\gamma g_t + \alpha g_t^{sam} + \alpha g_t^{meta}), \gamma = 1 - 2\alpha. \quad (20)$$

Suppose  $f$  is  $L$ -Lipschitz smooth. By the definitions of  $d_t = \theta_{t+1} - \theta_t$ ,  $f(\theta_t^{sam}) = f(\theta_t + \delta_t)$ , and  $f(\theta_t^{meta}) = f(\theta_t - \delta_t)$ , we have:

$$\begin{aligned} f(\theta_{t+1}) &\leq f(\theta_t) + \langle \nabla f(\theta_t), \theta_{t+1} - \theta_t \rangle + \frac{L}{2} \|\theta_{t+1} - \theta_t\|^2 \\ &= f(\theta_t) + \langle \nabla f(\theta_t), d_t \rangle + \frac{L}{2} \|d_t\|^2 \\ &= f(\theta_t) + \langle \nabla f(\theta_t), -\eta_t(\gamma g_t + \alpha g_t^{sam} + \alpha g_t^{meta}) \rangle \\ &\quad + \frac{L}{2} \|d_t\|^2. \end{aligned} \quad (21)$$

By the assumptions of  $\mathbb{E}[g_t] = \nabla f(\theta_t)$ ,  $\mathbb{E}[g_t^{sam}] = \nabla f(\theta_t^{sam})$ , and  $\mathbb{E}[g_t^{meta}] = \nabla f(\theta_t^{meta})$ , we take the expectation conditioned on the observations up to step  $t$  for both sides and then obtain:

$$\begin{aligned} \mathbb{E}[f(\theta_{t+1})] &\leq f(\theta_t) + \langle \nabla f(\theta_t), -\eta_t(\gamma \mathbb{E}[g_t] + \alpha \mathbb{E}[g_t^{sam}] \\ &\quad + \alpha \mathbb{E}[g_t^{meta}]) \rangle + \frac{L}{2} \mathbb{E}[\|d_t\|^2] \\ &= f(\theta_t) - \eta_t(\gamma \|\nabla f(\theta_t)\|^2 \\ &\quad + \alpha \langle \nabla f(\theta_t), \nabla f(\theta_t^{sam}) \rangle \\ &\quad + \alpha \langle \nabla f(\theta_t), \nabla f(\theta_t^{meta}) \rangle) + \frac{L}{2} \mathbb{E}[\|d_t\|^2]. \end{aligned} \quad (22)$$

Since perturbation  $\delta_t$  is small, by Taylor expansion,  $\nabla f(\theta_t^{sam})$  and  $\nabla f(\theta_t^{meta})$  can be approximated as:

$$\nabla f(\theta_t^{sam}) = \nabla f(\theta_t + \delta_t) \approx \nabla f(\theta_t) + \delta_t H(\theta_t), \quad (23)$$

and

$$\nabla f(\theta_t^{meta}) = \nabla f(\theta_t - \delta_t) \approx \nabla f(\theta_t) - \delta_t H(\theta_t), \quad (24)$$

where  $H(\theta_t)$  is the Hessian and the Taylor remainder is omitted. Plug Eq. (23) and Eq. (24) into Eq. (22), with the definition of  $\gamma = 1 - 2\alpha$ , we have:

$$\begin{aligned} \mathbb{E}[f(\theta_{t+1})] &\leq f(\theta_t) - \eta_t(\gamma + 2\alpha) \|\nabla f(\theta_t)\|^2 \\ &\quad - \eta_t \alpha \delta_t \langle \nabla f(\theta_t), H(\theta_t) \rangle \\ &\quad + \eta_t \alpha \delta_t \langle \nabla f(\theta_t), H(\theta_t) \rangle + \frac{L}{2} \mathbb{E}[\|d_t\|^2] \\ &= f(\theta_t) - \eta_t \|\nabla f(\theta_t)\|^2 + \frac{L}{2} \mathbb{E}[\|d_t\|^2]. \end{aligned} \quad (25)$$

Assume gradient is upper-bounded by  $G$ , Eq. (25) can be rewritten as:

$$\begin{aligned} \mathbb{E}[f(\theta_{t+1})] &\leq f(\theta_t) - \eta_t \|\nabla f(\theta_t)\|^2 + \frac{L}{2} \mathbb{E}[G^2 \eta_t^2] \\ &= f(\theta_t) - \eta_t \|\nabla f(\theta_t)\|^2 + \frac{L}{2} G^2 \eta_t^2. \end{aligned} \quad (26)$$

By re-arranging above formula, we have:

$$\eta_t \|\nabla f(\theta_t)\|^2 \leq f(\theta_t) - \mathbb{E}[f(\theta_{t+1})] + \frac{L}{2} G^2 \eta_t^2. \quad (27)$$

Perform telescope sum and take the expectation on each step  $t$ , we can obtain:

$$\sum_{t=1}^T \eta_t \|\nabla f(\theta_t)\|^2 \leq f(\theta_1) - \mathbb{E}[f(\theta_T)] + \frac{L}{2} G^2 \sum_{t=1}^T \eta_t^2. \quad (28)$$

By setting  $\eta_t = \frac{\eta_0}{\sqrt{t}}$ , we have:

$$\begin{aligned} \frac{\eta_0}{\sqrt{t}} \sum_{t=1}^T \|\nabla f(\theta_t)\|^2 &\leq f(\theta_1) - f_{min} + \frac{L}{2} G^2 \eta_0^2 \sum_{t=1}^T \frac{1}{t} \\ &\leq f(\theta_1) - f_{min} + \frac{L}{2} G^2 \eta_0^2 (1 + \log T). \end{aligned} \quad (29)$$

Hence

$$\frac{1}{T} \sum_{t=1}^T \|\nabla f(\theta_t)\|^2 \leq \frac{C_1 + C_2 \log T}{\sqrt{T}} \quad (30)$$

implies the convergence rate w.r.t.  $f(\theta)$  is  $O(\frac{\log T}{\sqrt{T}})$ , where  $C_1$  and  $C_2$  are some constants.

### A.3.2 Convergence W.R.T. Function $f(\theta^{sam})$

Denote the update  $d_t$  of the model parameter  $\theta$  at step  $t$  as:

$$d_t = -\eta_t(\gamma g_t + \alpha g_t^{sam} + \alpha g_t^{meta}), \gamma = 1 - 2\alpha. \quad (31)$$

Define  $d_t = \theta_{t+1} - \theta_t$ ,  $f(\theta_t^{sam}) = f(\theta_t + \delta_t)$ , and  $f(\theta_t^{meta}) = f(\theta_t - \delta_t)$ . By  $L$ -smoothness of  $f$ , we have:

$$\begin{aligned} f(\theta_{t+1}^{sam}) &\leq f(\theta_t^{sam}) + \langle \nabla f(\theta_t^{sam}), \theta_{t+1}^{sam} - \theta_t^{sam} \rangle \\ &\quad + \frac{L}{2} \|\theta_{t+1}^{sam} - \theta_t^{sam}\|^2 \\ &= f(\theta_t^{sam}) + \langle \nabla f(\theta_t^{sam}), \theta_{t+1} + \delta_{t+1} - \theta_t - \delta_t \rangle \\ &\quad + \frac{L}{2} \|\theta_{t+1} + \delta_{t+1} - \theta_t - \delta_t\|^2. \end{aligned} \quad (32)$$

According to the Cauchy-Schwarz inequality and AM-GM inequality, we re-arrange the above formula and then obtain:

$$\begin{aligned} f(\theta_{t+1}^{sam}) - f(\theta_t^{sam}) - \langle \nabla f(\theta_t^{sam}), d_t \rangle - L \|d_t\|^2 &\leq \\ \langle \nabla f(\theta_t^{sam}), \delta_{t+1} - \delta_t \rangle + L \|\delta_{t+1} - \delta_t\|^2. \end{aligned} \quad (33)$$

We first take the expectation conditioned on the observations up to step  $t$  for the  $LHS$ . By reusing results from Eq. (23) and Eq. (24), we have:

$$\begin{aligned} LHS &= \mathbb{E}[f(\theta_{t+1}^{sam})] - f(\theta_t^{sam}) - L \mathbb{E}[\|d_t\|^2] - \\ &\quad \langle \nabla f(\theta_t^{sam}), -\eta_t(\gamma \mathbb{E}[g_t] + \alpha \mathbb{E}[g_t^{sam}] + \alpha \mathbb{E}[g_t^{meta}]) \rangle \\ &= \mathbb{E}[f(\theta_{t+1}^{sam})] - f(\theta_t^{sam}) - L \mathbb{E}[\|d_t\|^2] + \\ &\quad \eta_t(\alpha \|\nabla f(\theta_t^{sam})\|^2 + \alpha \langle \nabla f(\theta_t^{sam}), \nabla f(\theta_t^{meta}) \rangle + \\ &\quad \gamma \langle \nabla f(\theta_t^{sam}), \nabla f(\theta_t) \rangle) \\ &\approx \mathbb{E}[f(\theta_{t+1}^{sam})] - f(\theta_t^{sam}) - L \mathbb{E}[\|d_t\|^2] + \\ &\quad \eta_t(\alpha \|\nabla f(\theta_t^{sam})\|^2 + \alpha \langle \nabla f(\theta_t^{sam}), \nabla f(\theta_t^{sam}) - \\ &\quad 2\delta_t H(\theta_t) \rangle + \gamma \langle \nabla f(\theta_t^{sam}), \nabla f(\theta_t^{sam}) - \delta_t H(\theta_t) \rangle) \\ &= \mathbb{E}[f(\theta_{t+1}^{sam})] - f(\theta_t^{sam}) - L \mathbb{E}[\|d_t\|^2] + \\ &\quad \eta_t(\|\nabla f(\theta_t^{sam})\|^2 - \langle \nabla f(\theta_t^{sam}), \delta_t H(\theta_t) \rangle) \\ &\geq \mathbb{E}[f(\theta_{t+1}^{sam})] - f(\theta_t^{sam}) + \eta_t \|\nabla f(\theta_t^{sam})\|^2 - \\ &\quad LG\rho_t \eta_t - LG^2 \eta_t^2, \end{aligned} \quad (34)$$

where the last inequality is due to (1) max eigenvalue of  $H$  is upper-bounded by  $L$ , (2) gradient is assumed to be upper-bounded by  $G$ , and (3) the definition of  $\delta_t$  that  $\delta_t = \rho_t \frac{g_t}{\|g_t\| + \epsilon}$  and  $\|\rho_t \frac{g_t}{\|g_t\| + \epsilon}\| < 1$ .

Inspired by [89], we take the expectation conditioned on the observations up to step  $t$  for the *RHS* of Eq. (43) and then obtain:

$$\begin{aligned}
RHS &= \langle \nabla f(\theta_t^{sam}), \mathbb{E}[\delta_{t+1} - \delta_t] \rangle + L\mathbb{E}[\|\delta_{t+1} - \delta_t\|^2] \\
&\leq G\rho_t \mathbb{E}\left[\left\|\frac{g_{t+1}}{g_{t+1} + \epsilon} - \frac{g_t}{g_t + \epsilon}\right\|\right] + \\
&\quad L\rho_t^2 \mathbb{E}\left[\left\|\frac{g_{t+1}}{g_{t+1} + \epsilon} - \frac{g_t}{g_t + \epsilon}\right\|^2\right] \\
&\leq G\rho_t \phi_t + L\rho_t^2 \phi_t^2,
\end{aligned} \tag{35}$$

where  $\phi_t$  denotes the angle between  $\nabla f(\theta_{t+1})$  and  $\nabla f(\theta_t)$ . According to the analysis in [89], when  $\eta_t$  and  $d_t$  are small,  $\phi_t$  is small and can be approximated as:

$$\phi_t \approx \tan(\phi) \approx \frac{\|H(\theta_t)d_t\|}{\|\nabla f(\theta_t)\|} \leq L\eta_t. \tag{36}$$

Plug Eq. (36) into Eq. (35), we have:

$$RHS \leq LG\rho_t\eta_t + L^3\rho_t^2\eta_t^2 \tag{37}$$

Combine Eq. (37) and Eq. (34), we have:

$$\begin{aligned}
\eta_t \|\nabla f(\theta_t^{sam})\|^2 &\leq f(\theta_t^{sam}) - \mathbb{E}[f(\theta_{t+1}^{sam})] + 2LG\rho_t\eta_t \\
&\quad + LG^2\eta_t^2 + L^3\rho_t^2\eta_t^2
\end{aligned} \tag{38}$$

By setting  $\eta_t = \frac{\eta_0}{\sqrt{t}}$  and  $\rho_t = \frac{\rho_0}{\sqrt{t}}$ , we perform telescope sum and take the expectation on each step  $t$ . Then we have:

$$\begin{aligned}
\sum_{t=1}^T \eta_t \|\nabla f(\theta_t^{sam})\|^2 &\leq f(\theta_1^{sam}) - \mathbb{E}[f(\theta_T^{sam})] + L^3\rho_0^2\eta_0^2 \sum_{t=1}^T \frac{1}{t^2} \\
&\quad + (2LG\rho_0\eta_0 + LG^2\eta_0^2) \sum_{t=1}^T \frac{1}{t} \\
\frac{\eta_0}{\sqrt{T}} \sum_{t=1}^T \|\nabla f(\theta_t^{sam})\|^2 &\leq f(\theta_1^{sam}) - f_{min} + \frac{\pi^2 L^3 \rho_0^2 \eta_0^2}{6} \\
&\quad + (2LG\rho_0\eta_0 + LG^2\eta_0^2)(1 + \log T),
\end{aligned} \tag{39}$$

Hence

$$\frac{1}{T} \sum_{t=1}^T \|\nabla f(\theta_t^{sam})\|^2 \leq \frac{C_3 + C_4 \log T}{\sqrt{T}} \tag{40}$$

implies the convergence rate w.r.t.  $f(\theta^{sam})$  is  $O(\frac{\log T}{\sqrt{T}})$ , where  $C_3$  and  $C_4$  are some constants.

### A.3.3 Convergence W.R.T. Function $f(\theta^{meta})$

Denote the update  $d_t$  of the model parameter  $\theta$  at step  $t$  as:

$$d_t = -\eta_t(\gamma g_t + \alpha g_t^{sam} + \alpha g_t^{meta}), \gamma = 1 - 2\alpha. \tag{41}$$

Define  $d_t = \theta_{t+1} - \theta_t$ ,  $f(\theta_t^{sam}) = f(\theta_t + \delta_t)$ , and  $f(\theta_t^{meta}) = f(\theta_t - \delta_t)$ . By  $L$ -smoothness of  $f$ , we have:

$$\begin{aligned}
f(\theta_{t+1}^{meta}) &\leq f(\theta_t^{meta}) + \langle \nabla f(\theta_t^{sam}), \theta_{t+1}^{meta} - \theta_t^{meta} \rangle \\
&\quad + \frac{L}{2} \|\theta_{t+1}^{meta} - \theta_t^{meta}\|^2 \\
&= f(\theta_t^{meta}) + \langle \nabla f(\theta_t^{meta}), \theta_{t+1} - \theta_t + \delta_t - \delta_{t+1} \rangle \\
&\quad + \frac{L}{2} \|\theta_{t+1} - \theta_t + \delta_t - \delta_{t+1}\|^2.
\end{aligned} \tag{42}$$

We re-arrange the above formula and then obtain:

$$\begin{aligned}
f(\theta_{t+1}^{meta}) - f(\theta_t^{meta}) - \langle \nabla f(\theta_t^{meta}), d_t \rangle - L\|d_t\|^2 &\leq \\
\langle \nabla f(\theta_t^{meta}), \delta_t - \delta_{t+1} \rangle + L\|\delta_t - \delta_{t+1}\|^2.
\end{aligned} \tag{43}$$

Similar to the proof in A.3.2, we take the expectation conditioned on the observations up to step  $t$  for the both sides and obtain:

$$\begin{aligned}
\mathbb{E}[f(\theta_{t+1}^{meta})] - f(\theta_t^{meta}) + \eta_t \|\nabla f(\theta_t^{meta})\|^2 &\leq \\
-LG^2\eta_t^2 &\leq L^3\rho_t^2\eta_t^2 \\
\eta_t \|\nabla f(\theta_t^{meta})\|^2 &\leq f(\theta_t^{meta}) - \mathbb{E}[f(\theta_{t+1}^{meta})] \\
&\quad + LG^2\eta_t^2 + L^3\rho_t^2\eta_t^2.
\end{aligned} \tag{44}$$

Following Eq. (39) and Eq. (40), we have:

$$\frac{1}{T} \sum_{t=1}^T \|\nabla f(\theta_t^{meta})\|^2 \leq \frac{C_5 + C_6 \log T}{\sqrt{T}}, \tag{45}$$

where  $C_5$  and  $C_6$  are some constants. Eq. (45) implies the convergence rate w.r.t.  $f(\theta^{meta})$  is  $O(\frac{\log T}{\sqrt{T}})$ .

### A.3.4 Convergence W.R.T. Overall Function $F(\theta)$

Note that we have proved convergence for  $f(\theta)$ ,  $f(\theta^{sam})$ , and  $f(\theta^{meta})$  in A.3.1, A.3.2, and A.3.3, respectively. By definition of  $F(\theta)$ , we have:

$$\begin{aligned}
\|\nabla F(\theta_t)\|^2 &= \|\gamma \nabla f(\theta_t) + \alpha \nabla f(\theta_t^{sam}) + \alpha \nabla f(\theta_t^{meta})\|^2 \\
&\leq \frac{10\gamma^2}{3} \|\nabla f(\theta_t)\|^2 + \frac{10\alpha^2}{3} \|\nabla f(\theta_t^{sam})\|^2 \\
&\quad + \frac{10\alpha^2}{3} \|\nabla f(\theta_t^{meta})\|^2.
\end{aligned} \tag{46}$$

Hence

$$\begin{aligned}
\frac{1}{T} \sum_{t=1}^T \|\nabla F(\theta_t)\|^2 &\leq \frac{10}{3T} (\gamma^2 \sum_{t=1}^T \|\nabla f(\theta_t)\|^2 + \\
&\quad \alpha^2 \sum_{t=1}^T \|\nabla f(\theta_t^{sam})\|^2 + \alpha^2 \sum_{t=1}^T \|\nabla f(\theta_t^{meta})\|^2)
\end{aligned} \tag{47}$$

also converges at rate  $O(\frac{\log T}{\sqrt{T}})$  since each item in the *RHS* converges at rate  $O(\frac{\log T}{\sqrt{T}})$ .

#### A.4. Proof of Proposition 3.5

By performing first-order Taylor expansion around  $\theta$ , we have:

$$\begin{aligned} f(\theta - \delta) &\approx f(\theta) - \delta \nabla f(\theta), \\ m(\theta - \delta) &\approx m(\theta) - \delta \nabla m(\theta), \end{aligned} \quad (48)$$

where the remainders are omitted. By assuming this proposition holds, we have:

$$\alpha(f(\theta - \delta) - f(\theta)) \approx \beta(m(\theta - \delta) - m(\theta)). \quad (49)$$

Applying Eq. (48) to Eq. (49), when the perturbation  $\delta$  is small, we can obtain:

$$\begin{aligned} -\alpha \delta \nabla f(\theta) &\approx \beta(m(\theta) - f(\theta)) - \beta \delta \nabla m(\theta) \\ f(\theta) - m(\theta) &\approx \delta \left( \frac{\alpha}{\beta} \nabla f(\theta) - \nabla m(\theta) \right) \\ \beta &\approx \alpha \frac{\nabla f(\theta)}{\nabla m(\theta) + \frac{C'}{\delta}}, \end{aligned} \quad (50)$$

where  $f(\theta) - m(\theta) \approx C'$  and  $C'$  is a small constant. For convenience, we set  $\beta$  as a hyperparameter, which meets the  $\beta \leq \alpha$  condition.

Table I. The optimal hyperparameter configurations for MeCAM on each dataset. The ‘lr’, ‘wd’, ‘dr’,  $\rho$ ,  $\alpha$ , and  $\beta$  denote the learning rate, the weight decay, the dropout rate, the perturbation radius, the weight for the surrogate gap of SAM, and the weight for the surrogate gap of meta-learning, respectively.

Dataset	lr	wd	dr	$\rho$	$\alpha$	$\beta$
PACS	$3e^{-5}$	$1e^{-4}$	0.5	0.1	0.1	0.1
VLCS	$1e^{-6}$	$1e^{-4}$	0.5	0.1	0.2	0.1
OfficeHome	$1e^{-5}$	$1e^{-4}$	0.5	0.2	0.2	0.1
TerraIncognita	$1e^{-5}$	$1e^{-4}$	0.5	0.01	0.05	0.05
DomainNet	$3e^{-5}$	$1e^{-6}$	0.5	0.1	0.2	0.1

## B. Optimal Hyperparameter Configurations

For a fair comparison, we followed the training and evaluation protocol in [23] to search for the optimal hyperparameters, where the test data information is unavailable. The search spaces of the learning rate (*i.e.*, ‘lr’), the perturbation radius  $\rho$ , the weight for the surrogate gap of SAM  $\alpha$ , and the weight for the surrogate gap of meta-learning  $\beta$  are  $\{1e^{-6}, 1e^{-5}, 3e^{-5}\}$ ,  $\{0.01, 0.05, 0.1, 0.2\}$ ,  $\{0.05, 0.1, 0.15, 0.2\}$ , and  $\{0.05, 0.1, 0.15, 0.2\}$ , respectively. For the weight decay (*i.e.*, ‘wd’) and the dropout rate (*i.e.*, ‘dr’), we inherited the optimal configurations in [75]. The optimal hyperparameter configurations for MeCAM on each dataset are provided in Table I. It is worth noting that all the optimal configurations also satisfy the condition  $\beta \leq \alpha$ .

## C. Full Results

In this section, we provide the detailed results of Table 2 and Table 3 in our manuscript. Specifically, we display the full results of our MeCAM and existing DG methods [4, 7, 13, 21, 26, 33, 39, 40, 43, 52, 56, 60, 62, 67, 69, 70, 77, 81, 85] on PACS, VLCS, OfficeHome, TerraIncognita, and DomainNet datasets in Table II, Table IV, Table VI, Table VIII, and Table X, respectively. We also display the full results of our MeCAM, optimizers [32, 47, 53, 79, 80, 88], and existing sharpness-based DG methods [20, 42, 75, 76, 82, 83] on PACS, VLCS, OfficeHome, TerraIncognita, and DomainNet datasets in Table III, Table V, Table VII, Table IX, and Table XI, respectively. The average accuracy and standard deviation, calculated across three trials with random seeds set to 0, 1, and 2, are reported for each method.

## D. Additional Experiments

### D.1. Extensibility Analysis

To evaluate the extensibility of our MeCAM, we integrated it with SWAD [9], which is a typical DG method based on ensemble learning, and repeated experiments on five DG datasets. The optimal hyperparameter configurations listed in Table B were directly applied to MeCAM. For SWAD, the hyperparameters were set to their default values: ‘n\_converge’=3, ‘n\_tolerance’=6, and ‘tolerance\_ratio’=0.3. Therefore, no additional hyperparameter search was performed. The results are presented in Table XII. It shows that our MeCAM integrated with SWAD outperforms other combinations on four datasets and also achieves the best overall performance, demonstrating the superior extensibility of our MeCAM.

### D.2. Ablation Study on Hyperparameters

Besides the vanilla training loss, the overall objective function of our MeCAM consists of the surrogate gap of SAM and the surrogate gap of meta-learning. There are three critical hyperparameters in MeCAM, where  $\rho$  controls the extent of perturbations and  $\alpha$  and  $\beta$  regulate the contributions of the surrogate gap of SAM and meta-learning, respectively. To explore the impact of these hyperparameters on MeCAM, we conducted additional ablation study on them, and the results are shown in Figure I. Figure I (a) shows that (1) the performance remains stable even with variations in  $\rho$  around 0.1; and (2) our MeCAM consistently outperforms SAM, with the exception of the case when  $\rho = 1.0$ , which leads to large perturbations. The results displayed in Figure I (b) indicate that (1) our MeCAM is robust to various  $\alpha$  and  $\beta$ , consistently achieving superior accuracy compared to SAM, even under the worst-case scenario; (2) setting  $\beta$  to 0.1 is a proper choice, as it yields the best or second-best performance across different values of  $\alpha$ ; and (3) setting

Table II. Full results ( $mean_{\pm std}$ ) of our MeCAM and existing DG methods calculated across three trials on PACS. The results denoted by † are taken from [75] and [13], while the results marked by ‡ are obtained directly from the original source.

Algorithm	Art	Cartoon	Photo	Sketch	Average
MMD† [40]	86.1 $\pm$ 1.4	79.4 $\pm$ 0.9	96.6 $\pm$ 0.2	76.5 $\pm$ 0.5	84.7
Mixstyle† [85]	86.8 $\pm$ 0.5	79.0 $\pm$ 1.4	96.6 $\pm$ 0.1	78.5 $\pm$ 2.3	85.2
GroupDRO† [62]	83.5 $\pm$ 0.9	79.1 $\pm$ 0.6	96.7 $\pm$ 0.3	78.3 $\pm$ 2.0	84.4
IRM† [4]	84.8 $\pm$ 1.3	76.4 $\pm$ 1.1	96.7 $\pm$ 0.6	76.1 $\pm$ 1.0	83.5
ARM† [81]	86.8 $\pm$ 0.6	76.8 $\pm$ 0.5	97.4 $\pm$ 0.3	79.3 $\pm$ 1.2	85.1
VREx† [33]	86.0 $\pm$ 1.6	79.1 $\pm$ 0.6	96.9 $\pm$ 0.5	77.7 $\pm$ 1.7	84.9
AND-mask† [56]	86.4 $\pm$ 1.1	80.8 $\pm$ 0.9	97.1 $\pm$ 0.2	81.3 $\pm$ 1.1	86.4
CDANN† [43]	84.6 $\pm$ 1.8	75.5 $\pm$ 0.9	96.8 $\pm$ 0.3	73.5 $\pm$ 0.6	82.6
DANN† [21]	86.4 $\pm$ 0.8	77.4 $\pm$ 0.8	97.3 $\pm$ 0.4	73.5 $\pm$ 2.3	83.7
RSC† [26]	85.4 $\pm$ 0.8	79.7 $\pm$ 1.8	97.6 $\pm$ 0.3	78.2 $\pm$ 1.2	85.2
MTL† [7]	87.5 $\pm$ 0.8	77.1 $\pm$ 0.5	96.4 $\pm$ 0.8	77.3 $\pm$ 1.8	84.6
Mixup† [77]	86.1 $\pm$ 0.5	78.9 $\pm$ 0.8	97.6 $\pm$ 0.1	75.8 $\pm$ 1.8	84.6
MLDG† [39]	85.5 $\pm$ 1.4	80.1 $\pm$ 1.7	97.4 $\pm$ 0.3	76.6 $\pm$ 1.1	84.9
ERM† [70]	84.7 $\pm$ 0.4	80.8 $\pm$ 0.6	97.2 $\pm$ 0.3	79.3 $\pm$ 1.0	85.5
SagNet† [52]	87.4 $\pm$ 1.0	80.7 $\pm$ 0.6	97.1 $\pm$ 0.1	80.0 $\pm$ 0.4	86.3
CORAL† [67]	88.3 $\pm$ 0.2	80.0 $\pm$ 0.5	97.5 $\pm$ 0.3	78.8 $\pm$ 1.3	86.2
Fishr† [60]	87.9 $\pm$ 0.6	80.8 $\pm$ 0.5	97.9 $\pm$ 0.4	81.1 $\pm$ 0.8	86.9
MADG† [13]	87.8 $\pm$ 0.5	82.2 $\pm$ 0.6	97.7 $\pm$ 0.3	78.3 $\pm$ 0.4	86.5
GMDG‡ [69]	84.7 $\pm$ 1.0	81.7 $\pm$ 2.4	97.5 $\pm$ 0.4	80.5 $\pm$ 1.8	85.6
MeCAM (Ours)	89.6 $\pm$ 0.6	83.3 $\pm$ 1.4	96.7 $\pm$ 0.3	83.5 $\pm$ 0.7	88.3

Table III. Full results ( $mean_{\pm std}$ ) of our MeCAM, optimizers, and existing sharpness-based DG methods calculated across three trials on PACS. Results marked with † and \* are inherited from [82] and obtained by reproduction, respectively.

Algorithm		Art	Cartoon	Photo	Sketch	Average
Optimizer	Adam† [32]	88.0 $\pm$ 1.2	79.7 $\pm$ 0.5	96.7 $\pm$ 0.4	72.7 $\pm$ 0.9	84.3
	AdamW† [47]	84.1 $\pm$ 1.5	80.7 $\pm$ 1.2	96.9 $\pm$ 0.4	72.8 $\pm$ 0.6	83.6
	SGD† [53]	85.1 $\pm$ 0.4	76.0 $\pm$ 0.3	98.3 $\pm$ 0.4	60.3 $\pm$ 6.1	79.9
	YOGI† [80]	84.4 $\pm$ 1.7	79.7 $\pm$ 0.6	95.8 $\pm$ 0.3	65.1 $\pm$ 1.5	81.2
	AdaBelief† [88]	85.4 $\pm$ 2.2	80.4 $\pm$ 1.1	97.4 $\pm$ 0.7	75.1 $\pm$ 1.4	84.6
	AdaHessian† [79]	88.4 $\pm$ 0.6	80.0 $\pm$ 0.9	97.7 $\pm$ 0.4	71.7 $\pm$ 4.1	84.5
Sharpness-based	SAM† [20]	85.7 $\pm$ 1.2	81.0 $\pm$ 1.4	97.1 $\pm$ 0.2	77.4 $\pm$ 1.8	85.3
	GAM† [83]	85.9 $\pm$ 0.9	81.3 $\pm$ 1.6	98.2 $\pm$ 0.4	79.0 $\pm$ 2.1	86.1
	SAGM* [75]	87.6 $\pm$ 0.4	81.8 $\pm$ 0.5	97.2 $\pm$ 0.1	81.3 $\pm$ 2.1	86.9
	FAD† [82]	88.5 $\pm$ 0.5	83.0 $\pm$ 0.8	98.4 $\pm$ 0.2	82.8 $\pm$ 0.9	88.2
	CRSAM* [76]	86.7 $\pm$ 0.5	80.5 $\pm$ 1.6	96.4 $\pm$ 0.5	77.8 $\pm$ 2.4	85.4
	FSAM* [42]	87.6 $\pm$ 1.1	80.2 $\pm$ 0.7	95.4 $\pm$ 0.4	82.8 $\pm$ 0.7	86.5
MeCAM (Ours)		89.6 $\pm$ 0.6	83.3 $\pm$ 1.4	96.7 $\pm$ 0.3	83.5 $\pm$ 0.7	88.3



Table IV. Full results ( $mean_{\pm std}$ ) of our MeCAM and existing DG methods calculated across three trials on VLCS. The results denoted by † are taken from [75] and [13], while the results marked by ‡ are obtained directly from the original source.

Algorithm	Caltech	LabelMe	SUN	VOC	Average
MMD <sup>†</sup> [40]	97.7 $\pm$ 0.1	64.0 $\pm$ 1.1	72.8 $\pm$ 0.2	75.3 $\pm$ 3.3	77.5
Mixstyle <sup>†</sup> [85]	98.6 $\pm$ 0.3	64.5 $\pm$ 1.1	72.6 $\pm$ 0.5	75.7 $\pm$ 1.7	77.9
GroupDRO <sup>†</sup> [62]	97.3 $\pm$ 0.3	63.4 $\pm$ 0.9	69.5 $\pm$ 0.8	76.7 $\pm$ 0.7	76.7
IRM <sup>†</sup> [4]	98.6 $\pm$ 0.1	64.9 $\pm$ 0.9	73.4 $\pm$ 0.6	77.3 $\pm$ 0.9	78.6
ARM <sup>†</sup> [81]	98.7 $\pm$ 0.2	63.6 $\pm$ 0.7	71.3 $\pm$ 1.2	76.7 $\pm$ 0.6	77.6
VREx <sup>†</sup> [33]	98.4 $\pm$ 0.3	64.4 $\pm$ 1.4	74.1 $\pm$ 0.4	76.2 $\pm$ 1.3	78.3
AND-mask <sup>†</sup> [56]	98.3 $\pm$ 0.3	64.5 $\pm$ 0.2	69.3 $\pm$ 1.3	73.4 $\pm$ 1.3	76.4
CDANN <sup>†</sup> [43]	97.1 $\pm$ 0.3	65.1 $\pm$ 1.2	70.7 $\pm$ 0.8	77.1 $\pm$ 1.5	77.5
DANN <sup>†</sup> [21]	99.0 $\pm$ 0.3	65.1 $\pm$ 1.4	73.1 $\pm$ 0.3	77.2 $\pm$ 0.6	78.6
RSC <sup>†</sup> [26]	97.9 $\pm$ 0.1	62.5 $\pm$ 0.7	72.3 $\pm$ 1.2	75.6 $\pm$ 0.8	77.1
MTL <sup>†</sup> [7]	97.8 $\pm$ 0.4	64.3 $\pm$ 0.3	71.5 $\pm$ 0.7	75.3 $\pm$ 1.7	77.2
Mixup <sup>†</sup> [77]	98.3 $\pm$ 0.6	64.8 $\pm$ 1.0	72.1 $\pm$ 0.5	74.3 $\pm$ 0.8	77.4
MLDG <sup>†</sup> [39]	97.4 $\pm$ 0.2	65.2 $\pm$ 0.7	71.0 $\pm$ 1.4	75.3 $\pm$ 1.0	77.2
ERM <sup>†</sup> [70]	98.0 $\pm$ 0.3	64.7 $\pm$ 1.2	71.4 $\pm$ 1.2	75.2 $\pm$ 1.6	77.3
SagNet <sup>†</sup> [52]	97.9 $\pm$ 0.4	64.5 $\pm$ 0.5	71.4 $\pm$ 1.3	77.5 $\pm$ 0.5	77.8
CORAL <sup>†</sup> [67]	98.3 $\pm$ 0.1	66.1 $\pm$ 1.2	73.4 $\pm$ 0.3	77.5 $\pm$ 1.2	78.8
Fislr <sup>†</sup> [60]	97.6 $\pm$ 0.7	67.3 $\pm$ 0.5	72.2 $\pm$ 0.9	75.7 $\pm$ 0.3	78.2
MADG <sup>†</sup> [13]	98.5 $\pm$ 0.2	65.8 $\pm$ 0.3	73.1 $\pm$ 0.3	77.3 $\pm$ 0.1	78.7
GMDG <sup>‡</sup> [69]	98.3 $\pm$ 0.4	65.9 $\pm$ 1.0	73.4 $\pm$ 0.8	79.3 $\pm$ 1.3	79.2
MeCAM (Ours)	99.5 $\pm$ 0.0	64.3 $\pm$ 0.5	75.2 $\pm$ 0.8	82.1 $\pm$ 0.3	80.3

Table V. Full results ( $mean_{\pm std}$ ) of our MeCAM, optimizers, and existing sharpness-based DG methods calculated across three trials on VLCS. Results marked with † and \* are inherited from [82] and obtained by reproduction, respectively.

Algorithm		Caltech	LabelMe	SUN	VOC	Average
Optimizer	Adam <sup>†</sup> [32]	98.9 $\pm$ 0.4	65.9 $\pm$ 1.5	71.0 $\pm$ 1.6	74.5 $\pm$ 2.0	77.3
	AdamW <sup>†</sup> [47]	98.3 $\pm$ 0.1	65.1 $\pm$ 1.7	70.9 $\pm$ 1.3	75.2 $\pm$ 1.5	77.4
	SGD <sup>†</sup> [53]	98.4 $\pm$ 0.2	64.7 $\pm$ 0.7	72.5 $\pm$ 0.8	76.6 $\pm$ 0.8	78.1
	YOGI <sup>†</sup> [80]	98.1 $\pm$ 0.7	63.9 $\pm$ 1.2	72.5 $\pm$ 1.6	75.7 $\pm$ 1.2	77.6
	AdaBelief <sup>†</sup> [88]	98.0 $\pm$ 0.1	63.9 $\pm$ 0.4	73.4 $\pm$ 1.0	78.2 $\pm$ 1.8	78.4
	AdaHessian <sup>†</sup> [79]	99.1 $\pm$ 0.3	65.0 $\pm$ 1.7	72.7 $\pm$ 1.3	77.7 $\pm$ 1.0	78.6
Sharpness-based	SAM <sup>†</sup> [20]	98.5 $\pm$ 1.0	66.2 $\pm$ 1.6	72.0 $\pm$ 1.0	76.1 $\pm$ 1.0	78.2
	GAM <sup>†</sup> [83]	98.8 $\pm$ 0.6	65.1 $\pm$ 1.2	72.9 $\pm$ 1.0	77.2 $\pm$ 1.9	78.5
	SAGM* [75]	98.4 $\pm$ 0.6	65.1 $\pm$ 1.1	74.1 $\pm$ 0.5	78.6 $\pm$ 2.4	79.1
	FAD <sup>†</sup> [82]	99.1 $\pm$ 0.5	66.8 $\pm$ 0.9	73.6 $\pm$ 1.0	76.1 $\pm$ 1.3	78.9
	CRSAM* [76]	99.0 $\pm$ 0.4	63.7 $\pm$ 0.8	73.8 $\pm$ 0.5	79.8 $\pm$ 1.4	79.1
	FSAM* [42]	98.9 $\pm$ 0.2	64.5 $\pm$ 0.4	74.1 $\pm$ 1.0	80.0 $\pm$ 1.0	79.4
MeCAM (Ours)		99.5 $\pm$ 0.0	64.3 $\pm$ 0.5	75.2 $\pm$ 0.8	82.1 $\pm$ 0.3	80.3

Table VI. Full results ( $mean_{\pm std}$ ) of our MeCAM and existing DG methods calculated across three trials on OfficeHome. The results denoted by † are taken from [75] and [13], while the results marked by ‡ are obtained directly from the original source.

Algorithm	Art	Clipart	Product	Real-World	Average
MMD† [40]	60.4 $\pm$ 0.2	53.3 $\pm$ 0.3	74.3 $\pm$ 0.1	77.4 $\pm$ 0.6	66.4
Mixstyle† [85]	51.1 $\pm$ 0.3	53.2 $\pm$ 0.4	68.2 $\pm$ 0.7	69.2 $\pm$ 0.6	60.4
GroupDRO† [62]	60.4 $\pm$ 0.7	52.7 $\pm$ 1.0	75.0 $\pm$ 0.7	76.0 $\pm$ 0.7	66.0
IRM† [4]	58.9 $\pm$ 2.3	52.2 $\pm$ 1.6	72.1 $\pm$ 2.9	74.0 $\pm$ 2.5	64.3
ARM† [81]	58.9 $\pm$ 0.8	51.0 $\pm$ 0.5	74.1 $\pm$ 0.1	75.2 $\pm$ 0.3	64.8
VREx† [33]	60.7 $\pm$ 0.9	53.0 $\pm$ 0.9	75.3 $\pm$ 0.1	76.6 $\pm$ 0.5	66.4
AND-mask† [56]	60.3 $\pm$ 0.5	52.3 $\pm$ 0.6	75.1 $\pm$ 0.2	76.6 $\pm$ 0.3	66.1
CDANN† [43]	61.5 $\pm$ 1.4	50.4 $\pm$ 2.4	74.4 $\pm$ 0.9	76.6 $\pm$ 0.8	65.7
DANN† [21]	59.9 $\pm$ 1.3	53.0 $\pm$ 0.3	73.6 $\pm$ 0.7	76.9 $\pm$ 0.5	65.9
RSC† [26]	60.7 $\pm$ 1.4	51.4 $\pm$ 0.3	74.8 $\pm$ 1.1	75.1 $\pm$ 1.3	65.5
MTL† [7]	61.5 $\pm$ 0.7	52.4 $\pm$ 0.6	74.9 $\pm$ 0.4	76.8 $\pm$ 0.4	66.4
Mixup† [77]	62.4 $\pm$ 0.8	54.8 $\pm$ 0.6	76.9 $\pm$ 0.3	78.3 $\pm$ 0.2	68.1
MLDG† [39]	61.5 $\pm$ 0.9	53.2 $\pm$ 0.6	75.0 $\pm$ 1.2	77.5 $\pm$ 0.4	66.8
ERM† [70]	61.3 $\pm$ 0.7	52.4 $\pm$ 0.3	75.8 $\pm$ 0.1	76.6 $\pm$ 0.3	66.5
SagNet† [52]	63.4 $\pm$ 0.2	54.8 $\pm$ 0.4	75.8 $\pm$ 0.4	78.3 $\pm$ 0.3	68.1
CORAL† [67]	65.3 $\pm$ 0.4	54.4 $\pm$ 0.5	76.5 $\pm$ 0.1	78.4 $\pm$ 0.5	68.7
Fishr† [60]	63.4 $\pm$ 0.8	54.2 $\pm$ 0.3	76.4 $\pm$ 0.3	78.5 $\pm$ 0.2	68.2
MADG† [13]	68.6 $\pm$ 0.5	55.5 $\pm$ 0.2	79.6 $\pm$ 0.3	81.5 $\pm$ 0.4	71.3
GMDG‡ [69]	68.9 $\pm$ 0.3	56.2 $\pm$ 1.7	79.9 $\pm$ 0.6	82.0 $\pm$ 0.4	70.7
MeCAM (Ours)	65.9 $\pm$ 0.6	58.7 $\pm$ 0.5	77.1 $\pm$ 0.5	79.9 $\pm$ 0.3	70.4

Table VII. Full results ( $mean_{\pm std}$ ) of our MeCAM, optimizers, and existing sharpness-based DG methods calculated across three trials on OfficeHome. Results marked with † and \* are inherited from [82] and obtained by reproduction, respectively.

Algorithm		Art	Clipart	Product	Real-World	Average
Optimizer	Adam† [32]	63.9 $\pm$ 0.8	48.1 $\pm$ 0.6	77.0 $\pm$ 0.9	81.8 $\pm$ 1.6	67.6
	AdamW† [47]	66.1 $\pm$ 0.7	48.7 $\pm$ 0.6	76.6 $\pm$ 0.8	83.6 $\pm$ 0.4	68.8
	SGD† [53]	65.3 $\pm$ 0.8	48.8 $\pm$ 1.4	76.7 $\pm$ 0.3	83.0 $\pm$ 0.7	68.5
	YOGI† [80]	63.5 $\pm$ 1.0	49.2 $\pm$ 1.2	76.2 $\pm$ 0.5	84.5 $\pm$ 0.6	68.3
	AdaBelief† [88]	65.6 $\pm$ 2.0	48.1 $\pm$ 0.9	74.8 $\pm$ 0.8	83.6 $\pm$ 0.9	68.0
	AdaHessian† [79]	63.0 $\pm$ 2.9	50.0 $\pm$ 1.4	77.7 $\pm$ 0.8	83.0 $\pm$ 0.5	68.4
Sharpness-based	SAM† [20]	63.5 $\pm$ 1.2	48.6 $\pm$ 0.9	77.0 $\pm$ 0.8	82.9 $\pm$ 1.3	68.0
	GAM† [83]	63.0 $\pm$ 1.2	49.8 $\pm$ 0.5	77.6 $\pm$ 0.6	82.4 $\pm$ 1.0	68.2
	SAGM* [75]	64.2 $\pm$ 0.6	56.2 $\pm$ 0.4	78.2 $\pm$ 0.2	79.2 $\pm$ 0.1	69.4
	FAD† [82]	63.5 $\pm$ 1.0	50.3 $\pm$ 0.8	78.0 $\pm$ 0.4	85.0 $\pm$ 0.6	69.2
	CRSAM* [76]	60.8 $\pm$ 3.7	56.9 $\pm$ 0.4	78.3 $\pm$ 0.5	79.5 $\pm$ 0.7	68.9
	FSAM* [42]	64.7 $\pm$ 0.3	57.3 $\pm$ 0.8	78.8 $\pm$ 0.1	79.9 $\pm$ 0.2	70.2
MeCAM (Ours)		65.9 $\pm$ 0.6	58.7 $\pm$ 0.5	77.1 $\pm$ 0.5	79.9 $\pm$ 0.3	70.4

Table VIII. Full results ( $mean_{\pm std}$ ) of our MeCAM and existing DG methods calculated across three trials on TerraIncognita. The results denoted by † are taken from [75] and [13], while the results marked by ‡ are obtained directly from the original source.

Algorithm	L100	L38	L43	L46	Average
MMD† [40]	41.9 $\pm$ 3:0	34.8 $\pm$ 1:0	57.0 $\pm$ 1:9	35.2 $\pm$ 1:8	42.2
Mixstyle† [85]	54.3 $\pm$ 1:1	34.1 $\pm$ 1:1	55.9 $\pm$ 1:1	31.7 $\pm$ 2:1	44.0
GroupDRO† [62]	41.2 $\pm$ 0:7	38.6 $\pm$ 2:1	56.7 $\pm$ 0:9	36.4 $\pm$ 2:1	43.2
IRM† [4]	54.6 $\pm$ 1:3	39.8 $\pm$ 1:9	56.2 $\pm$ 1:8	39.6 $\pm$ 0:8	47.6
ARM† [81]	49.3 $\pm$ 0:7	38.3 $\pm$ 2:4	55.8 $\pm$ 0:8	38.7 $\pm$ 1:3	45.5
VREx† [33]	48.2 $\pm$ 4:3	41.7 $\pm$ 1:3	56.8 $\pm$ 0:8	38.7 $\pm$ 3:1	46.4
AND-mask† [56]	54.7 $\pm$ 1:8	48.4 $\pm$ 0:5	55.1 $\pm$ 0:5	41.3 $\pm$ 0:6	49.8
CDANN† [43]	47.0 $\pm$ 1:9	41.3 $\pm$ 4:8	54.9 $\pm$ 1:7	39.8 $\pm$ 2:3	45.8
DANN† [21]	51.1 $\pm$ 3:5	40.6 $\pm$ 0:6	57.4 $\pm$ 0:5	37.7 $\pm$ 1:8	46.7
RSC† [26]	50.2 $\pm$ 2:2	39.2 $\pm$ 1:4	56.3 $\pm$ 1:4	40.8 $\pm$ 0:6	46.6
MTL† [7]	49.3 $\pm$ 1:2	39.6 $\pm$ 6:3	55.6 $\pm$ 1:1	37.8 $\pm$ 0:8	45.6
Mixup† [77]	59.6 $\pm$ 2:0	42.2 $\pm$ 1:4	55.9 $\pm$ 0:8	33.9 $\pm$ 1:4	47.9
MLDG† [39]	54.2 $\pm$ 3:0	44.3 $\pm$ 1:1	55.6 $\pm$ 0:3	36.9 $\pm$ 2:2	47.8
ERM† [70]	54.3 $\pm$ 0:4	42.5 $\pm$ 0:7	55.6 $\pm$ 0:3	38.8 $\pm$ 2:5	47.8
SagNet† [52]	53.0 $\pm$ 2:9	43.0 $\pm$ 2:5	57.9 $\pm$ 0:6	40.4 $\pm$ 1:3	48.6
CORAL† [67]	51.6 $\pm$ 2:4	42.2 $\pm$ 1:0	57.0 $\pm$ 1:0	39.8 $\pm$ 2:9	47.7
Fishr† [60]	60.4 $\pm$ 0:9	50.3 $\pm$ 0:3	58.8 $\pm$ 0:5	44.9 $\pm$ 0:5	53.6
MADG† [13]	60.0 $\pm$ 1:2	51.8 $\pm$ 0:2	57.4 $\pm$ 0:3	45.6 $\pm$ 0:5	53.7
GMDG‡ [69]	60.9 $\pm$ 4:4	47.3 $\pm$ 2:8	55.2 $\pm$ 0:9	41.0 $\pm$ 2:4	51.1
MeCAM (Ours)	55.6 $\pm$ 1:4	40.8 $\pm$ 3:6	58.5 $\pm$ 0:5	40.5 $\pm$ 1:6	48.9

Table IX. Full results ( $mean_{\pm std}$ ) of our MeCAM, optimizers, and existing sharpness-based DG methods calculated across three trials on TerraIncognita. Results marked with † and \* are inherited from [82] and obtained by reproduction, respectively.

Algorithm		L100	L38	L43	L46	Average
Optimizer	Adam† [32]	42.2 $\pm$ 3:4	40.7 $\pm$ 1:2	59.9 $\pm$ 0:2	35.0 $\pm$ 2:8	44.4
	AdamW† [47]	44.2 $\pm$ 6:8	39.8 $\pm$ 1:9	60.3 $\pm$ 2:0	36.6 $\pm$ 1:8	45.2
	SGD† [53]	41.8 $\pm$ 5:8	39.8 $\pm$ 3:9	60.5 $\pm$ 2:2	37.5 $\pm$ 1:1	44.9
	YOGI† [80]	43.9 $\pm$ 2:2	42.5 $\pm$ 2:6	60.5 $\pm$ 1:1	34.8 $\pm$ 1:6	45.4
	AdaBelief† [88]	42.6 $\pm$ 6:7	43.0 $\pm$ 2:0	60.2 $\pm$ 1:3	35.1 $\pm$ 0:3	45.2
	AdaHessian† [79]	42.5 $\pm$ 4:8	39.5 $\pm$ 1:0	58.4 $\pm$ 2:6	37.3 $\pm$ 0:8	44.4
Sharpness-based	SAM† [20]	42.9 $\pm$ 3:5	43.0 $\pm$ 2:2	60.5 $\pm$ 1:6	36.4 $\pm$ 1:2	45.7
	GAM† [83]	42.2 $\pm$ 2:6	42.9 $\pm$ 1:7	60.2 $\pm$ 1:8	35.5 $\pm$ 0:7	45.2
	SAGM* [75]	52.2 $\pm$ 3:9	42.3 $\pm$ 0:2	59.9 $\pm$ 0:3	39.9 $\pm$ 2:2	48.6
	FAD† [82]	44.3 $\pm$ 2:2	43.5 $\pm$ 1:7	60.9 $\pm$ 2:0	34.1 $\pm$ 0:5	45.7
	CRSAM* [76]	50.8 $\pm$ 0:5	35.3 $\pm$ 1:1	56.8 $\pm$ 0:1	38.4 $\pm$ 1:4	45.3
	FSAM* [42]	47.7 $\pm$ 3:1	39.3 $\pm$ 3:6	57.8 $\pm$ 1:7	39.5 $\pm$ 2:1	46.1
MeCAM (Ours)		55.6 $\pm$ 1:4	40.8 $\pm$ 3:6	58.5 $\pm$ 0:5	40.5 $\pm$ 1:6	48.9

Table X. Full results ( $mean_{\pm std}$ ) of our MeCAM and existing DG methods calculated across three trials on DomainNet. The results denoted by † are taken from [75] and [13], while the results marked by ‡ are obtained directly from the original source.

Algorithm	Clip	Info	Paint	Quick	Real	Sketch	Average
MMD† [40]	32.1 $\pm$ 13.3	11.0 $\pm$ 4.6	26.8 $\pm$ 11.3	8.7 $\pm$ 2.1	32.7 $\pm$ 13.8	28.9 $\pm$ 11.9	23.4
Mixstyle† [85]	51.9 $\pm$ 0.4	13.3 $\pm$ 0.2	37.0 $\pm$ 0.5	12.3 $\pm$ 0.1	46.1 $\pm$ 0.3	43.4 $\pm$ 0.4	34.0
GroupDRO† [62]	47.2 $\pm$ 0.5	17.5 $\pm$ 0.4	33.8 $\pm$ 0.5	9.3 $\pm$ 0.3	51.6 $\pm$ 0.4	40.1 $\pm$ 0.6	33.3
IRM† [4]	48.5 $\pm$ 2.8	15.0 $\pm$ 1.5	38.3 $\pm$ 4.3	10.9 $\pm$ 0.5	48.2 $\pm$ 5.2	42.3 $\pm$ 3.1	33.9
ARM† [81]	49.7 $\pm$ 0.3	16.3 $\pm$ 0.5	40.9 $\pm$ 1.1	9.4 $\pm$ 0.1	53.4 $\pm$ 0.4	43.5 $\pm$ 0.4	35.5
VREx† [33]	47.3 $\pm$ 3.5	16.0 $\pm$ 1.5	35.8 $\pm$ 4.6	10.9 $\pm$ 0.3	49.6 $\pm$ 4.9	42.0 $\pm$ 3.0	33.6
AND-mask† [56]	52.3 $\pm$ 0.8	17.3 $\pm$ 0.5	43.7 $\pm$ 1.1	12.3 $\pm$ 0.4	55.8 $\pm$ 0.4	46.1 $\pm$ 0.8	37.9
CDANN† [43]	54.6 $\pm$ 0.4	17.3 $\pm$ 0.1	43.7 $\pm$ 0.9	12.1 $\pm$ 0.7	56.2 $\pm$ 0.4	45.9 $\pm$ 0.5	38.3
DANN† [21]	53.1 $\pm$ 0.2	18.3 $\pm$ 0.1	44.2 $\pm$ 0.7	11.8 $\pm$ 0.1	55.5 $\pm$ 0.4	46.8 $\pm$ 0.6	38.3
RSC† [26]	55.0 $\pm$ 1.2	18.3 $\pm$ 0.5	44.4 $\pm$ 0.6	12.2 $\pm$ 0.2	55.7 $\pm$ 0.7	47.8 $\pm$ 0.9	38.9
MTL† [7]	57.9 $\pm$ 0.5	18.5 $\pm$ 0.4	46.0 $\pm$ 0.1	12.5 $\pm$ 0.1	59.5 $\pm$ 0.3	49.2 $\pm$ 0.1	40.6
Mixup† [77]	55.7 $\pm$ 0.3	18.5 $\pm$ 0.5	44.3 $\pm$ 0.5	12.5 $\pm$ 0.4	55.8 $\pm$ 0.3	48.2 $\pm$ 0.5	39.2
MLDG† [39]	59.1 $\pm$ 0.2	19.1 $\pm$ 0.3	45.8 $\pm$ 0.7	13.4 $\pm$ 0.3	59.6 $\pm$ 0.2	50.2 $\pm$ 0.4	41.2
ERM† [70]	62.8 $\pm$ 0.4	20.2 $\pm$ 0.3	50.3 $\pm$ 0.3	13.7 $\pm$ 0.5	63.7 $\pm$ 0.2	52.1 $\pm$ 0.5	43.8
SagNet† [52]	57.7 $\pm$ 0.3	19.0 $\pm$ 0.2	45.3 $\pm$ 0.3	12.7 $\pm$ 0.5	58.1 $\pm$ 0.5	48.8 $\pm$ 0.2	40.3
CORAL† [67]	59.2 $\pm$ 0.1	19.7 $\pm$ 0.2	46.6 $\pm$ 0.3	13.4 $\pm$ 0.4	59.8 $\pm$ 0.2	50.1 $\pm$ 0.6	41.5
Fishr† [60]	58.3 $\pm$ 0.5	20.2 $\pm$ 0.2	47.9 $\pm$ 0.2	13.6 $\pm$ 0.3	60.5 $\pm$ 0.3	50.5 $\pm$ 0.3	41.8
MADG† [13]	62.5 $\pm$ 0.4	22.0 $\pm$ 0.3	34.1 $\pm$ 0.3	15.1 $\pm$ 0.2	57.4 $\pm$ 1.1	48.0 $\pm$ 0.3	39.9
GMDG‡ [69]	63.4 $\pm$ 0.3	22.4 $\pm$ 0.4	51.4 $\pm$ 0.4	13.4 $\pm$ 0.8	64.4 $\pm$ 0.3	52.4 $\pm$ 0.4	44.6
MeCAM (Ours)	64.2 $\pm$ 0.2	21.5 $\pm$ 0.4	51.6 $\pm$ 0.2	14.2 $\pm$ 0.6	63.9 $\pm$ 0.1	54.6 $\pm$ 0.3	45.0

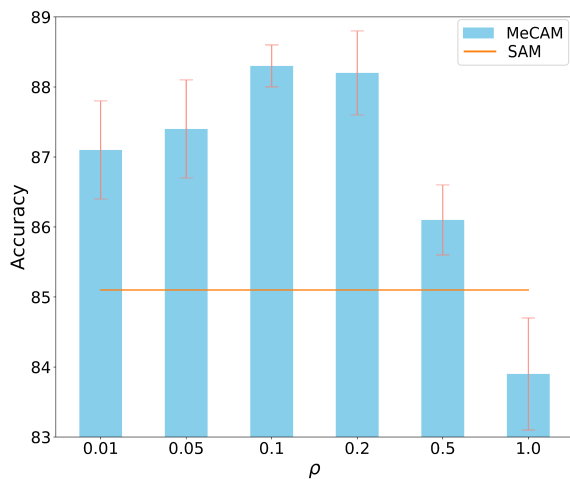
Table XI. Full results ( $mean_{\pm std}$ ) of our MeCAM, optimizers, and existing sharpness-based DG methods calculated across three trials on DomainNet. Results marked with † and \* are inherited from [82] and obtained by reproduction, respectively.

Algorithm		Clip	Info	Paint	Quick	Real	Sketch	Average
Optimizer	Adam† [32]	63.0 $\pm$ 0.3	20.2 $\pm$ 0.4	49.1 $\pm$ 0.1	13.0 $\pm$ 0.3	62.0 $\pm$ 0.4	50.7 $\pm$ 0.1	43.0
	AdamW† [47]	63.0 $\pm$ 0.6	20.6 $\pm$ 0.2	49.6 $\pm$ 0.0	13.0 $\pm$ 0.2	63.6 $\pm$ 0.2	50.4 $\pm$ 0.1	43.4
	SGD† [53]	61.3 $\pm$ 0.2	20.4 $\pm$ 0.2	49.4 $\pm$ 0.2	12.6 $\pm$ 0.1	65.7 $\pm$ 0.0	49.6 $\pm$ 0.2	43.2
	YOGI† [80]	63.3 $\pm$ 0.1	20.6 $\pm$ 0.1	50.1 $\pm$ 0.3	13.2 $\pm$ 0.3	62.8 $\pm$ 0.1	51.0 $\pm$ 0.2	43.5
	AdaBelief† [88]	63.5 $\pm$ 0.2	20.5 $\pm$ 0.1	50.0 $\pm$ 0.3	13.2 $\pm$ 0.3	63.1 $\pm$ 0.1	50.7 $\pm$ 0.1	43.5
	AdaHessian† [79]	63.3 $\pm$ 0.2	21.4 $\pm$ 0.1	50.8 $\pm$ 0.3	13.6 $\pm$ 0.1	65.7 $\pm$ 0.1	51.4 $\pm$ 0.2	44.4
Sharpness-based	SAM† [20]	63.3 $\pm$ 0.1	20.3 $\pm$ 0.3	50.0 $\pm$ 0.3	13.6 $\pm$ 0.2	63.6 $\pm$ 0.3	49.6 $\pm$ 0.4	43.4
	GAM† [83]	63.0 $\pm$ 0.5	20.2 $\pm$ 0.2	50.3 $\pm$ 0.1	13.2 $\pm$ 0.3	64.5 $\pm$ 0.2	51.6 $\pm$ 0.5	43.8
	SAGM* [75]	63.6 $\pm$ 0.5	21.6 $\pm$ 0.2	51.4 $\pm$ 0.4	14.2 $\pm$ 0.3	64.2 $\pm$ 0.2	53.1 $\pm$ 0.2	44.7
	FAD† [82]	64.1 $\pm$ 0.3	21.9 $\pm$ 0.2	50.6 $\pm$ 0.3	14.2 $\pm$ 0.4	63.6 $\pm$ 0.1	52.2 $\pm$ 0.2	44.4
	CRSAM* [76]	62.9 $\pm$ 0.3	20.7 $\pm$ 0.2	50.8 $\pm$ 0.2	15.2 $\pm$ 0.4	62.5 $\pm$ 0.4	53.5 $\pm$ 0.2	44.3
	FSAM* [42]	63.3 $\pm$ 0.5	21.5 $\pm$ 0.1	51.6 $\pm$ 0.3	15.4 $\pm$ 0.5	63.5 $\pm$ 0.2	54.3 $\pm$ 0.2	44.9
MeCAM (Ours)		64.2 $\pm$ 0.2	21.5 $\pm$ 0.4	51.6 $\pm$ 0.2	14.2 $\pm$ 0.6	63.9 $\pm$ 0.1	54.6 $\pm$ 0.3	45.0

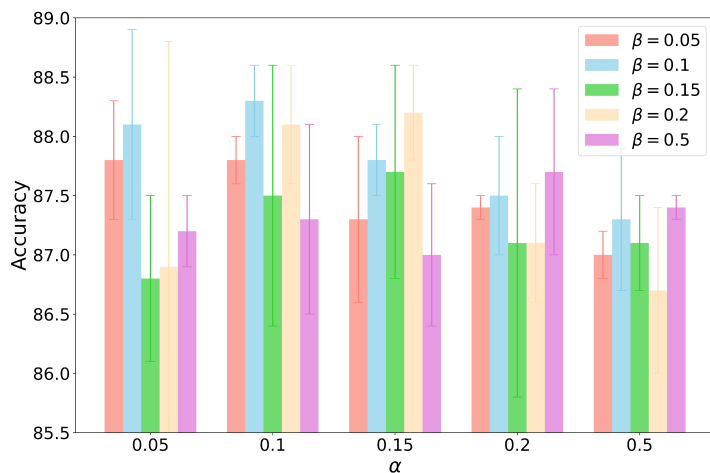
both  $\alpha$  and  $\beta$  to 0.1 leads to the best overall performance on PACS dataset with a competitive standard deviation.

Table XII. Performance of our MeCAM, three optimizers, and FAD integrated with SWAD on five public DG datasets. The best results are highlighted in **bold**. The results denoted by † are inherited from [82].

Algorithm	PACS	VLCS	OfficeHome	TerraInc	DomainNet	Average
Adam + SWAD†	86.8	79.1	70.1	46.5	44.1	65.3
AdamW + SWAD†	87.0	78.5	70.8	46.9	45.0	65.6
SGD + SWAD†	85.2	79.1	71.0	46.7	42.8	65.0
FAD + SWAD†	88.5	<b>79.8</b>	<b>71.8</b>	47.5	45.0	66.5
MeCAM (Ours) + SWAD	<b>88.9</b>	<b>79.8</b>	70.8	<b>48.9</b>	<b>45.9</b>	<b>66.9</b>



(a) Ablation Study on  $\rho$



(b) Ablation Study on  $\alpha$  and  $\beta$

Figure I. Accuracy of our MeCAM with various  $\rho$ ,  $\alpha$ , and  $\beta$  on the PACS dataset. (a) We evaluated our MeCAM using different  $\rho$ . (b) We conducted the grid search for  $\alpha$  and  $\beta$ .